Effect of phase noise on useful quantum correlations in Bose Josephson junctions

G. Ferrini,[1, *] D. Spehner,[1, 2] A. Minguzzi,[1] and F.W.J. Hekking[1]

[1]*Université Grenoble 1 and CNRS, Laboratoire de Physique et Modélisation*
des Milieux Condensés UMR5493, B.P. 166, 38042 Grenoble, France
[2]*Université Grenoble 1 and CNRS, Institut Fourier UMR5582, B.P. 74, 38402 Saint Martin d'Hères, France*
(Dated: August 10, 2018)

In a two-mode Bose Josephson junction the dynamics induced by a sudden quench of the tunnel amplitude leads to the periodic formation of entangled states. For instance, squeezed states are formed at short times and macroscopic superpositions of phase states at later times. The two modes of the junction can be viewed as the two arms of an interferometer; use of entangled states allows to perform atom interferometry beyond the classical limit. Decoherence due to the presence of noise degrades the quantum correlations between the atoms, thus reducing phase sensitivity of the interferometer. We consider the noise induced by stochastic fluctuations of the energies of the two modes of the junction. We analyze its effect on squeezed states and macroscopic superpositions and study quantitatively the amount of quantum correlations which can be used to enhance the phase sensitivity with respect to the classical limit. To this aim we compute the squeezing parameter and the quantum Fisher information during the quenched dynamics. For moderate noise intensities we show that these useful quantum correlations increase on time scales beyond the squeezing regime. This suggests multicomponent superpositions as interesting candidates for high-precision atom interferometry.

PACS numbers: 03.75.-b,03.75.Mn

I. INTRODUCTION

Confined ultracold atomic gases are promising candidates for implementing quantum simulators and for applications in quantum technology, due to the high controllability of the experimental parameters such as the atomic interactions [1] and the geometry of the trap [2, 3]. Among the applications we cite high-sensitivity atom interferometry, which can be used for enhancing the precision in atomic clocks and in magnetic field sensors [4–7]. Of particular interest are Bose Josephson junctions formed by two modes of a Bose-Einstein condensate. The modes may correspond either to two internal states of the condensed atoms in a single potential well or to two spatially separated wavefunctions in a double well. During the dynamics following a sudden quench of the tunnel amplitude connecting the two modes, squeezed states are formed at early times. It has been shown theoretically [8–10] and experimentally [6, 7] that these states can be used to estimate phase shifts with sensitivity below the shot noise limit, the limit one obtains using classical states. The highest possible phase sensitivity, limited by quantum uncertainty only, can be achieved by using macroscopic superpositions of e.g. atomic phase states [11, 12]. Such superpositions are however formed at later times during the quenched dynamics of the BJJ [13–15]. They are expected to be very fragile with respect to decoherence effects caused by particle losses [16], collisions with thermal atoms [17, 18], interaction with the electromagnetic field [19], and random fluctuations of the trapping potential [20].

In this work we consider the effects of phase noise on the states formed during the quenched dynamics of the BJJ. Phase noise is induced by stochastic fluctuations of the energies of the two modes of the BJJ. Together with atom losses, such a noise is one of the main sources of decoherence in the experiments of Refs. [6, 7, 21]. Interestingly, macroscopic superpositions of phase states in BJJs have been shown to be robust with respect to phase noise, their decoherence rate being independent of the total number of atoms in the condensate [22]. Below we show that these long-lived states can be useful in interferometry to improve phase sensitivity. In particular, we compare the best possible phase sensitivity obtained with the state of the BJJ at the times of formation of macroscopic superpositions to the one obtained at earlier times when squeezed states are produced. This allows us to determine which are the most useful quantum states for interferometric applications in the presence of phase noise. In order to quantify the amount of quantum correlations useful for interferometry, we calculate the quantum Fisher information. In the theory of estimation of an unknown parameter, this quantity is related to the bound on the precision with which the unknown parameter - in interferometry, the phase shift - can be determined [12, 23]. We show that for moderate noise intensities the quantum Fisher information at the time of formation of the first superpositions of phase states exceeds the one found at the time at which squeezed states appear. In other words, despite the action of phase noise, a better phase sensitivity can be reached by using states produced at times later than the time for optimal squeezing.

The paper is organized as follows. In Sec.II we recall the definition of the two parameters relevant in interfer-
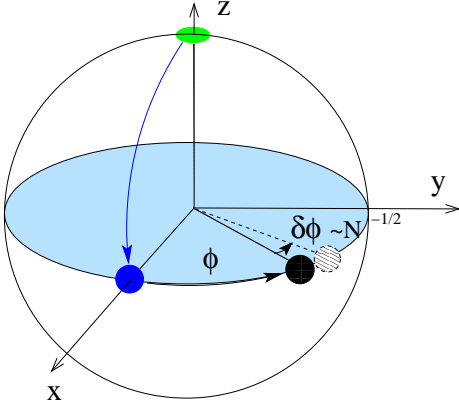
FIG. 1. (Color online) Rotations on the Bloch sphere in the interferometric scheme: the input coherent state at the north pole (green disk) is rotated around the y-axis by an angle $\pi/2$ (blue disk) and afterwards around the z-axis by the unkown phase φ (black disk). The precision $\Delta\varphi$ on the estimation of φ is larger than the size $\sqrt{N}/2$ of the disk, representing the angular momentum fluctuations, divided by the radius $N/2$ of the sphere. The last rotation around the y-axis is not represented.

ometry, i.e. the coherent spin squeezing and the quantum Fisher information, and link them to multiparticle entanglement. In Sec.III we present the model which describes the quenched time evolution of a BJJ both in the absence and in the presence of noise. A peculiarity of the quenched time evolution is the formation of multicomponent superpositions of phase states, and we illustrate the effect of phase noise on those states in Sec.IV by calculating a suitable probability distribution. In Sec.V we compute the coherent spin squeezing and the quantum Fisher information during the quenched dynamics of the BJJ, first in the absence and then in the presence of noise, and study quantitatively the loss of useful correlations as a function of time. Finally, Sec. VI contains some concluding remarks.

II. PHASE ESTIMATION IN ATOM INTERFEROMETRY

A. Phase estimation and the quantum Fisher information

The goal in interferometry is to estimate an unknown phase shift φ with the highest possible precision. In atom interferometry, an input state is first transformed into a superposition of two modes, analogous to the two arms of an optical interferometer. These modes acquire distinct phases φ_1 and φ_2 during the subsequent quantum evolution. They are are finally recombined to read out interference fringes, from which the phase difference $\varphi = \varphi_1 - \varphi_2$ is inferred. The interferometric sequence can be described by means of rotation matrices acting on the two-mode vector state, that is, by SU(2) rotation matrices in

the Schwinger representation [24, 25]. The generators of the rotations are the angular-momentum operators $\hat{J}_x$, $\hat{J}_y$, and $\hat{J}_z$, related to the annihilation operator $\hat{a}_j$ of an atom in the mode $j = 1, 2$ by $\hat{J}_x = (\hat{a}_1^\dagger \hat{a}_2 + \hat{a}_2^\dagger \hat{a}_1)/2$, $\hat{J}_y = -i(\hat{a}_1^\dagger \hat{a}_2 - \hat{a}_2^\dagger \hat{a}_1)/2$, and $\hat{J}_z \equiv \hat{n} = (\hat{a}_1^\dagger \hat{a}_1 - \hat{a}_2^\dagger \hat{a}_2)/2$, the latter being the number imbalance operator. Let us consider the case where the two modes correspond to two internal states of the atoms in an optically trapped Bose-Einstein condensate. The total number N of atoms in the condensate is assumed to be fixed and all atoms are initially in the lower energy state (mode $j = 1$). The input state is then $|n_z = N/2\rangle$, where $|n_z = n\rangle \equiv |n_1, n_2\rangle$ denotes the Fock state satisfying $\hat{J}_z|n_z = n\rangle = n|n_z = n\rangle$, $n_1 = N/2 + n$ and $n_2 = N/2 - n$ being the number of atoms in the lower and upper modes, respectively. The application of a $\pi/2$ laser pulse with frequency in resonance with the two internal levels plays the role of a beam splitter in optical interferometers. It brings the input state onto the coherent state $|\theta = \pi/2, \phi = 0\rangle$, where the SU(2) coherent states are defined as [26]

$$|\theta, \phi\rangle = \sum_{n_1=0}^{N} \binom{N}{n_1}^{1/2} \frac{\alpha^{n_1}}{(1+|\alpha|^2)^{N/2}} |n_1, N - n_1\rangle \quad (1)$$

with $\alpha = \tan(\theta/2)\exp(-i\phi)$. It is easy to show that $|\theta, \phi\rangle \propto (e^{-i\phi}\sin(\theta/2)a_1^\dagger + \cos(\theta/2)a_2^\dagger)^N|0\rangle$ (here $|0\rangle$ is the vacuum state), meaning that all atoms occupy the same one-atom state. A coherent state can be visualized as a disc of diameter $\sqrt{N}/2$ on the Bloch sphere of radius $N/2$, centered at $N(\sin\theta\cos\phi, \sin\theta\sin\phi, -\cos\theta)/2$. The coordinates of the center are the expectation values of the angular momentum operators $\hat{J}_x$, $\hat{J}_y$, and $\hat{J}_z$ in $|\theta, \phi\rangle$, whereas the diameter of the disc gives the quantum fluctuations of $\hat{J}_{\vec{n}} = \vec{J} \cdot \vec{n}$ in the directions $\vec{n}$ tangential to the sphere. The coherent states with $\theta = \pi/2$ on the equator of the Bloch sphere are referred to as *phase states*. The Fock state $|n_z = N/2\rangle$ is a coherent state with $\theta = \pi$, located at the north pole of the Bloch sphere. The action of the beam splitter is therefore a rotation of the atomic state around the y-axis by an angle of $\pi/2$ radians, leading to the phase state $|\theta = \pi/2, \phi = 0\rangle$. Then the state is rotated around the z-axis by the free evolution, the phase accumulation being due to a different energy shift between the two states. This rotation is the analog of the different phase paths in the two arms of an optical interferometer. The consecutive rotations of the input state on the Bloch sphere are represented in Fig.1. Finally, by recombining the two paths, the state is rotated again around the y-axis by an angle of $-\pi/2$ radians. The interferometric sequence can thus be described by a succession of three rotations, and the output state of the linear interferometer is

$$|\psi_{\text{out}}\rangle = e^{-i\frac{\pi}{2}\hat{J}_y} e^{-i\varphi\hat{J}_z} e^{i\frac{\pi}{2}\hat{J}_y}|\psi_{\text{in}}\rangle = e^{-i\varphi\hat{J}_x}|\psi_{\text{in}}\rangle, \quad (2)$$

where $|\psi_{\text{in}}\rangle$ is the input state, assumed here to be pure. More generally, the output state of the interferometer is

$$\hat{\rho}_{\text{out}}(\varphi) = e^{-i\varphi\hat{J}_{\vec{n}}} \hat{\rho}_{\text{in}} e^{i\varphi\hat{J}_{\vec{n}}}. \quad (3)$$

where $\hat{\rho}_{\text{in}}$ is the input density matrix and $\vec{n}$ the unit vector representing the effective rotation axis associated to a given interferometric sequence.

In a typical experiment one has access to the probability distribution associated to the operator $\hat{J}_z$ measured with respect to the output state. This quantum distribution depends on the phase shift φ. The latter is then determined by means of a statistical estimator depending on the results of the measurements of $\hat{J}_z$ in the output state. The precision $\Delta\varphi$ with which the phase shift φ can be determined depends on the chosen estimator, on the input state and on the measurement performed on the output state. Optimizing over all possible measurements, the best precision that can be achieved for a given input state $\hat{\rho}_{\text{in}}$ is, according to the Cramér-Rao bound [23],

$$\Delta\varphi \geq (\Delta\varphi)_{\text{best}} = \frac{1}{\sqrt{m}\sqrt{F_Q\left[\hat{\rho}_{\text{in}}, \hat{J}_{\vec{n}}\right]}}, \qquad (4)$$

where m is the number of measurements and $F_Q[\hat{\rho}_{\text{in}}, \hat{J}_{\vec{n}}]$ the quantum Fisher information given by [23]

$$F_Q\left[\hat{\rho}_{\text{in}}, \hat{J}_{\vec{n}}\right] = 2 \sum_{l,m,p_l+p_m>0} \frac{(p_l - p_m)^2}{p_l + p_m}|\langle l|\hat{J}_{\vec{n}}|m\rangle|^2, \quad (5)$$

$\{|l\rangle\}$ being an orthonormal basis diagonalizing $\hat{\rho}_{\text{in}} = \sum_l p_l|l\rangle\langle l|$ (with $p_l \geq 0$ and $\sum_l p_l = 1$). The Fisher information (5) depends on the input state and on the direction $\vec{n}$ of the interferometer. It has the meaning of the square of a "statistical speed" at which the state evolves along the curve defined by Eq.(3) in the space of density matrices when the parameter φ is varied [11, 23]: if one increases φ starting from $\varphi = 0$ with a fixed velocity $\dot{\varphi}$, the faster the state (3) becomes distinguishable from $\hat{\rho}_{\text{in}}$, the larger is its quantum Fisher information F_Q. Hence the bound (5) relates the problem of estimating a phase shift in an interferometer to the problem of distinguishing neighbouring quantum states [23]. Indeed, the quantum Fisher information is related to the Bures riemannian distance on the space of density matrices [27].

For pure input states $|\psi_{\text{in}}\rangle$, the quantum Fisher information is given by the quantum fluctuation $(\Delta J_{\vec{n}})^2 = \langle\psi_{\text{in}}|\hat{J}_{\vec{n}}^2|\psi_{\text{in}}\rangle - \langle\psi_{\text{in}}|\hat{J}_{\vec{n}}|\psi_{\text{in}}\rangle^2$ of $\hat{J}_{\vec{n}}$,

$$F_Q\left[|\psi_{\text{in}}\rangle, \hat{J}_{\vec{n}}\right] = 4(\Delta J_{\vec{n}})^2. \qquad (6)$$

This allows to reinterpret the Cramér-Rao lower bound (4) as a generalized uncertainty principle

$$\Delta\varphi\,\Delta J_{\vec{n}} \geq \frac{1}{2\sqrt{m}}, \qquad (7)$$

in which the generator $\hat{J}_{\vec{n}}$ of the transformation (3) and the phase shift φ play the role of two conjugate variables - φ being here not an observable but a parameter [23]. For instance, the Fisher information of a phase state $|\psi_{\text{in}}\rangle = |\theta = \pi/2, \phi\rangle$ in the directions $\vec{n} = \vec{e}_x$,

$\vec{e}_y$, and $\vec{e}_z$ are equal to $N\sin^2\phi$, $N\cos^2\phi$, and N, respectively. According to (7), for such a state the best precision that can be achieved on the phase shift is $(\Delta\varphi)_{\text{best}} = 1/\sqrt{Nm} \equiv (\Delta\varphi)_{SN}$, corresponding to the *shot-noise limit* of independent atoms.

The saturation of the bound (4) requires both a suitable classical post-processing on the m outcomes of the measurements (e.g. the maximum likelihood estimation in the limit of large m [23]) and the knowledge of the optimum observable to measure. This latter task can be difficult as the optimum measurement may depend on the phase shift itself [28].

It can be shown [11, 12] that for any separable input state $\hat{\rho}_{\text{in}}$, $F_Q[\hat{\rho}_{\text{in}}, \hat{J}_{\vec{n}}] \leq N$, so that

$$F_Q\left[\hat{\rho}_{\text{in}}, \hat{J}_{\vec{n}}\right] > N \qquad (8)$$

is a sufficient condition for $\hat{\rho}_{\text{in}}$ to be entangled; in other words, $F_Q - N$ is an entanglement witness. By Eq.(4), the inequality (8) is a necessary and sufficient condition for sub-shot noise sensitivity $(\Delta\varphi)_{\text{best}} < (\Delta\varphi)_{SN}$. In what follows, the input states leading to such a condition are called *useful states* for interferometry (or, more briefly, "useful states"). It is worthwhile to stress that the inequality (8) is not a necessary condition for entanglement: indeed, there exists entangled states which are not useful for interferometry, that is, with a Fisher information $F_Q \leq N$ [11, 29].

The quantum Fisher information is bounded by N^2. This is easy to show for pure states by noticing that the largest square fluctuation of $\hat{J}_{\vec{n}}$ in Eq.(6) is smaller or equal to $N^2/4$ (see [12]); for mixed states this follows from the convexity of F_Q (see [11]). According to Eq.(4), the best sensitivity that can be achieved in linear interferometers [30] is then $(\Delta\varphi)_{\text{best}} = (\Delta\varphi)_{HL} \equiv 1/N$. This corresponds to the so-called *Heisenberg limit*. This limit is reached using highly entangled atoms as input state, e.g. the macroscopic superposition given by the so-called NOON state $|\psi_{\text{NOON}}\rangle = (|N,0\rangle + e^{i\alpha}|0,N\rangle)/\sqrt{2}$, with α being a real phase. The quantum Fisher information of a NOON state is equal to N^2 in the direction $\vec{n} = \vec{e}_z$. It is instructive to compare this result with the value of the quantum Fisher information for a statistical mixture of the same states, $\hat{\rho}_{\text{NONO}} = (|N,0\rangle\langle N,0| + |0,N\rangle\langle 0,N|)/2$. The latter is found with the help of Eq.(5) to be equal to N in all directions $\vec{n}$ in the (xOy)-plane and to vanish in the direction $\vec{e}_z$. Therefore, the scaling of F_Q like N^2 for $\hat{\rho}_{\text{NOON}} = |\psi_{\text{NOON}}\rangle\langle\psi_{\text{NOON}}|$ is due to the presence of the off-diagonal terms $\hat{\rho}_{\text{NOON}} - \hat{\rho}_{\text{NONO}} = (e^{-i\alpha}|N,0\rangle\langle 0,N| + e^{i\alpha}|0,N\rangle\langle N,0|)/2$.

To summarize, the study of the quantum Fisher information and its scaling with the number of atoms allows to quantify the amount of quantum correlations which can be used to enhance the precision on the phase shift in interferometry.

Phase estimation	Entanglement
$F_Q\left[\hat{\rho}_{\rm in}\right] > N \Leftrightarrow (\Delta\varphi)_{\rm best} < (\Delta\varphi)_{SN}$	$F_Q\left[\hat{\rho}_{\rm in}\right] > N \Rightarrow \hat{\rho}_{\rm in} \neq \hat{\rho}_{\rm sep}$
$\xi^2\left[\hat{\rho}_{\rm in}\right] < 1 \Rightarrow (\Delta\varphi)_{\rm best} < (\Delta\varphi)_{SN}$	$\xi^2\left[\hat{\rho}_{\rm in}\right] < 1 \Rightarrow \hat{\rho}_{\rm in} \neq \hat{\rho}_{\rm sep}$

TABLE I. Necessary and/or sufficient conditions for sub-shot noise phase sensitivity in an atom interferometer and multi-particle entanglement in terms of the quantum Fisher information and spin-squeezing parameter.

B. Coherent spin squeezing

Atomic squeezed states are examples of nonclassical states useful for interferometry, which have been recently realized experimentally [4–7]. The coherent spin squeezing parameter quantifies the angular-momentum fluctuations along the direction $\vec{n}$ [9, 10] according to

$$\xi_{\vec{n}}^2\left[\hat{\rho}_{\rm in}, \hat{J}_{\vec{n}}\right] = \frac{N\Delta^2 \hat{J}_{\vec{n}}}{\langle \hat{J}_{\vec{p}_1}\rangle^2 + \langle \hat{J}_{\vec{p}_2}\rangle^2}, \qquad (9)$$

where

$$\begin{aligned}\vec{p}_1 &= \cos\phi\, \vec{e}_x + \sin\phi\, \vec{e}_y \\ \vec{p}_2 &= -\cos\theta\sin\phi\, \vec{e}_x + \cos\theta\cos\phi\, \vec{e}_y + \sin\theta\, \vec{e}_z\end{aligned} \quad (10)$$

are unit vectors perpendicular to

$$\vec{n} = \sin\theta\sin\phi\, \vec{e}_x - \sin\theta\cos\phi\, \vec{e}_y + \cos\theta\, \vec{e}_z, \qquad (11)$$

and $\langle\cdot\rangle = {\rm tr}(\cdot\hat{\rho}_{\rm in})$ is the mean expectation in state $\hat{\rho}_{\rm in}$. A state $\hat{\rho}_{\rm in}$ is said to be squeezed in the direction $\vec{n}$ if the squeezing parameter satisfies

$$\xi_{\vec{n}}^2\left[\hat{\rho}_{\rm in}, \hat{J}_{\vec{n}}\right] < 1. \qquad (12)$$

It is known that Eq.(12) provides both a sufficient (but not necessary) condition for sub-shot noise sensitivity [10] and a sufficient (but not necessary) condition for entanglement of $\hat{\rho}_{\rm in}$ [9]. We remark that the squeezing criterion (12) does not recognize all useful states in interferometry. For instance, the NOON state does not fulfill this criterium even though it leads to the best achievable precision. The criteria for entanglement and sub-shot noise sensitivity are summarized in Table I.

C. Optimum coherent spin squeezing and quantum Fisher information

The quantum Fisher information F_Q and the spin squeezing parameter ξ introduced in the previous subsections depend on the direction of the generator which defines the interferometric sequence (3). For instance, as shown in Sec.II A, $F_Q[|\psi_{\rm NOON}\rangle, \hat{J}_z] = N^2$, corresponding to a maximally entangled state, whereas in the perpendicular directions $F_Q[|\psi_{\rm NOON}\rangle, \hat{J}_x] = F_Q[|\psi_{\rm NOON}\rangle, \hat{J}_y] = N$. Hence, in order to quantify the useful correlations of

a quantum state, one needs to optimize F_Q and ξ over all the possible directions by defining [29]

$$\xi^2\left[\hat{\rho}_{\rm in}\right] \equiv \min_{\vec{n}} \xi_{\vec{n}}^2\left[\hat{\rho}_{\rm in}\right] \;,\; F_Q\left[\hat{\rho}_{\rm in}\right] \equiv \max_{\vec{n}} F_Q\left[\hat{\rho}_{\rm in}, \hat{J}_{\vec{n}}\right]. \qquad (13)$$

Let us consider the 3×3 real symmetric covariance matrix $\gamma[\hat{\rho}_{\rm in}]$ with matrix elements

$$\gamma_{ij}\left[\hat{\rho}_{\rm in}\right] = \frac{1}{2} \sum_{l,m,p_l+p_m>0} \frac{(p_l - p_m)^2}{p_l + p_m} \Re{\rm e}\left[\langle l|\hat{J}_i|m\rangle\langle m|\hat{J}_j|l\rangle\right] \qquad (14)$$

where $\{|l\rangle\}$ is the orthonormal eigenbasis of $\hat{\rho}_{\rm in}$ as in Eq.(5). According to standard linear algebra, the maximum of $F_Q[\hat{\rho}_{\rm in}, \hat{J}_{\vec{n}}] = 4(\vec{n}, \gamma\left[\hat{\rho}_{\rm in}\right]\vec{n})$ over all unit vectors $\vec{n}$ is equal to

$$F_Q\left[\hat{\rho}_{\rm in}\right] = 4\gamma_{\max}, \qquad (15)$$

$\gamma_{\max}$ being the largest eigenvalue of the matrix $\gamma[\hat{\rho}_{\rm in}]$. In the following it will be useful to define also the matrix

$$G_{ij}[\hat{\rho}] \equiv \frac{1}{2}\langle \hat{J}_i\hat{J}_j + \hat{J}_j\hat{J}_i\rangle - \langle\hat{J}_i\rangle\langle\hat{J}_j\rangle, \qquad (16)$$

where $\langle\dots\rangle = {\rm tr}(\dots\hat{\rho})$, with $\hat{\rho}$ being the system density matrix. Note that for pure input states $|\psi_{\rm in}\rangle$ the matrix $\gamma_{ij}[|\psi_{\rm in}\rangle]$ reduces to the matrix $G_{ij}[|\psi_{\rm in}\rangle\langle\psi_{\rm in}|]$, which is easier to compute than the more general expression (14). The optimum quantum Fisher information is then given (up to a factor four) by the largest uncertainty of the angular momentum operators $\hat{J}_{\vec{n}}$ (see Eq.(6)). For the sake of brevity, in the following we will omit both the adjective "optimum" and the explicit dependence on the input state, designating the optimum coherent spin squeezing and the optimum quantum Fisher information respectively by ξ^2 and F_Q, unless where source of confusion.

III. QUENCHED DYNAMICS OF A BJJ

A. Noiseless dynamics

We describe a Bose Josephson junction (BJJ) by a two-mode Hamiltonian [31], which in terms of the angular-momentum operators introduced in Sec.II reads

$$\hat{H}^{(0)} = \chi\hat{J}_z^2 - \lambda\hat{J}_z - 2K\hat{J}_x. \qquad (17)$$

This Hamiltonian models both a single-component Bose gas trapped in a double-well potential [21] - external BJJ - and a binary mixture of atoms in distinct hyperfine states trapped in a single well [6, 32] - internal BJJ. In the external BJJ the two modes i correspond to the lowest-energy spatial modes in each well. For the internal BJJ, the two relevant modes are the two hyperfine states. The first term in the Hamiltonian (17) describes the repulsive atom-atom interactions; for the external BJJ, χ is half the sum of the interaction energies U_i in the two modes,

whereas for the internal BJJ $\chi = (U_1 + U_2)/2 - U_{12}$ also depends on the inter-species interaction U_{12}. In both cases, $\lambda = \Delta E + (N-1)(U_2 - U_1)/2$ is related to the difference $\Delta E = E_2 - E_1$ between the energies of the two modes. The last term in (17) corresponds to tunnelling between the two wells or, for the internal BJJ, to a resonant laser field coupling the two hyperfine states, which can serve to implement a 50% beam splitter as described in Sec.II A. Both χ and K are experimentally tunable parameters. In internal BJJs arbitrary rotations of the form (3) can be performed with a suitable combination of laser pulses. Such rotations are typically realized fast enough to neglect the non-linear effects induced by the interactions [6]. The residual effect of interactions on the interferometric sequence has been recently addressed in Refs. [33, 34].

We consider the dynamical evolution induced by a sudden quench of the tunnel amplitude K to zero, taking as initial state the phase state $|\theta = \pi/2, \phi = 0\rangle$. This is the ground state of the Hamiltonian (17) in the regime $KN \gg \chi$ where tunelling dominates interactions (in the internal BJJ this state can be produced by using a laser pulse as explained in Sec.II A). We assume a fixed total number of atoms N, that is, we do not account for atom losses. Going to the rotating frame [35], we may suppose that $\lambda = 0$. In the absence of noise, the atomic state

$$|\psi^{(0)}(t)\rangle = e^{-i\chi \hat{J}_z^2 t}|\theta = \pi/2, \phi = 0\rangle \qquad (18)$$

displays a periodic evolution with period $T = 2\pi/\chi$ if N is even and $T/2$ if N is odd, corresponding to the revival time. At intermediate times the dynamics drives the system first into a squeezed state at short times, then at times $t_q = \pi/(\chi q)$ to a macroscopic superposition of q phase states given by [13–15]

$$|\psi^{(0)}(t_q)\rangle = u_0 \sum_{k=0}^{q-1} c_{k,q}\left|\frac{\pi}{2}, \phi_{k,q}\right\rangle \qquad (19)$$

where $|u_0| = q^{-1/2}$, $\phi_{k,q} = (2k - N)\frac{\pi}{q}$, $c_{k,q} = e^{i\pi k^2/q}$ if q is even, and $\phi_{k,q} = (2k + 1 - N)\frac{\pi}{q}$, $c_{k,q} = e^{i\pi k(k+1)/q}$ if q is odd. This follows from Eqs.(1) and (18) and the use of the Fourier expansion $e^{-i\pi n_1^2/q} = u_0 \sum_{k=0}^{q-1} e^{i\pi k^2/q} e^{-2i\pi n_1 k/q}$. As in the case of the NOON state discussed in Sec.II A, the two-component superposition formed at $t = t_2 = T/4$ leads to the best achievable phase sensitivity if used as an input state of the interferometer described by Eq.(3) [11]. We will show in Sec.II that the multicomponent superpositions with $3 \leq q \lesssim \sqrt{N}$, which are formed at earlier times $t_q < t_2$, lead to comparable phase sensitivities up to a factor of two. The fact that squeezed states and macroscopic superpositions of phase states are intrinsically produced by interatomic interactions yields a major advantage of atomic interferometers over optical ones.

B. Dynamics of a noisy BJJ

The presence of noise during the dynamical evolution of the BJJ affects the preparation of the aforementioned useful entangled states [37]. We focus here on phase noise caused by a randomly fluctuating energy difference $\Delta E(t)$ between the two modes, assuming that the interaction energies U_1 and U_2 are not fluctuating. In the single-well experiment [6] (internal BJJ), such a noise is induced by fluctuations of the magnetic field, whereas in the double-well experiment [21] (external BJJ) it is induced by fluctuations in direction of the laser beam producing the double-well potential with respect to the trapping potential. The corresponding time evolution which follows the sudden quench $K \to 0$ is described by the time-dependent Hamiltonian

$$\hat{H}(t) = \chi \hat{J}_z^2 - \lambda(t)\hat{J}_z. \qquad (20)$$

Even in presence of noise, the time evolution following the quench can be exactly integrated since the noise term $\lambda(t)\hat{J}_z$ commutes with the noiseless Hamiltonian $\chi \hat{J}_z^2$ [22]. For a given realization of the stochastic process $\lambda(t)$, the state of the atoms at time t is

$$|\psi(t)\rangle = e^{-i\phi(t)\hat{J}_z}|\psi^{(0)}(t)\rangle \qquad (21)$$

where $\phi(t) \equiv -\int_0^t d\tau \lambda(\tau)$ and $|\psi^{(0)}(t)\rangle$ is the time-evolved state (18) in the absence of noise. The system density matrix is then obtained by $\hat{\rho}(t) = \overline{|\psi(t)\rangle\langle\psi(t)|} = \int dP[\lambda]|\psi(t)\rangle\langle\psi(t)|$, where the overline denotes the average over the noise realizations. The introduction of the distribution probability for the random angle $\phi(t)$,

$$f(\phi, t) = \int dP[\lambda(t)]\,\delta(\phi - \phi(t)) \qquad (22)$$

allows to write it as

$$\hat{\rho}(t) = \int_{-\infty}^{\infty} d\phi\, f(\phi, t)\, e^{-i\phi\hat{J}_z}\hat{\rho}^{(0)}(t)e^{i\phi\hat{J}_z}, \qquad (23)$$

where $\hat{\rho}^{(0)}(t) = |\psi^{(0)}(t)\rangle\langle\psi^{(0)}(t)|$ is the density matrix in the absence of noise. Under the hypothesis of a gaussian noise (see Appendix A) the probability distribution (22) reads

$$f(\phi, t) = \frac{1}{\sqrt{2\pi}a(t)}e^{-\frac{(\phi + \overline{\lambda}t)^2}{2a^2(t)}}, \qquad (24)$$

where $\overline{\lambda} = \overline{\Delta E} + (N-1)(U_2 - U_1)/2$ and the variance $a^2(t)$ is given in terms of the noise correlation function

$$h(\tau - \tau') = \overline{\lambda(\tau)\lambda(\tau')} - \overline{\lambda}^2 = \overline{\Delta E(\tau)\Delta E(\tau')} - \overline{\Delta E}^2 \quad (25)$$

by

$$a^2(t) = \int_0^t d\tau \int_0^t d\tau' h(\tau - \tau'). \qquad (26)$$

We note that h depends only on the time difference $\tau - \tau'$ by the stationarity of the stochastic process $\lambda(t)$, which also implies $\overline{\lambda(t)} = \overline{\lambda(0)} \equiv \overline{\lambda}$; moreover, h decreases to zero at sufficiently long times. By projecting Eq.(23) on the Fock basis $\{|n_z = n\rangle\}$ we obtain

$$\langle n_z = n|\hat{\rho}(t)|n_z = n'\rangle = e^{-\frac{a^2(t)(n-n')^2}{2}} e^{i\overline{\lambda}t(n-n')}$$
$$\times \langle n_z = n|\hat{\rho}^{(0)}(t)|n_z = n'\rangle. \quad (27)$$

In order to discuss the effect of the phase noise on the state of the atoms we briefly discuss the noise variance $a(t)$. We first notice that under our hypothesis, $a(t)$ and thus the decoherence factor (given by the first exponential in the right-hand side of Eq.(27)) is independent of the number of atoms N in the BJJ. This is in contrast with the usual scenario for decoherence which predicts stronger decoherence as the number of particles in the system is increased. As a consequence of this fact, macroscopic superpositions of the form (19) are robust against phase noise, as was shown in [22] and will be detailed in Sec.IV below.

Let us denote by t_c the largest time such that $h(\tau) \simeq h(0) = \delta\lambda(0)^2 \equiv \delta\lambda^2$ and by T_c the characteristic time at which $h(\tau)$ vanishes. If the time evolution occurs on a short scale such that $t < t_c$ then the colored nature of the noise plays an important role and

$$a^2(t) \simeq \delta\lambda^2 t^2. \quad (28)$$

If instead the time evolution occurs on a time scale much larger than the noise correlation time T_c we obtain the same result as for white noise,

$$a^2(t) \simeq 2t \int_0^\infty h(y)dy, \quad (29)$$

which corresponds to the Markov approximation.

The effect of phase noise can be partially suppressed by using the so-called spin-echo protocol [36]. This strategy was followed in a recent experiment [6]. The analysis discussed in this section can be adapted to take into account the residual effect of phase noise when spin echo pulses are applied, see Appendix B.

IV. EFFECT OF PHASE NOISE ON MULTICOMPONENT MACROSCOPIC SUPERPOSITIONS OF PHASE STATES

Before analyzing the Fisher information and the spin squeezing during the quenched dynamics discussed above in detail, we wish to study the nature of the state of the atoms under phase noise at the specific times t_q which in the noiseless BJJ correspond to the formation of multi-component superpositions of phase states. We first illustrate the effect of the noise on the structure of the density matrix, then we study a suitable probability distribution which is particularly sensible to decoherence.

A. Structure of the density matrix in the Fock basis

In the absence of noise the quenched dynamics of the Bose Josephson junction leads to the formation of coherent superpositions with q components as given by Eq.(19). The corresponding density matrix $\hat{\rho}^{(0)}(t_q) = |\psi^{(0)}(t_q)\rangle\langle\psi^{(0)}(t_q)|$ has the form $\hat{\rho}^{(0)}(t_q) = \sum_{k,k'} \hat{\rho}^{(0)}_{kk'}(t_q)$, where the indices k and k' label the various components of the superposition and $\hat{\rho}^{(0)}_{kk'}(t_q) = q^{-1}c_{k,q}c^*_{k',q}|\pi/2, \phi_{k,q}\rangle\langle\pi/2, \phi_{k',q}|$. For general decoherence processes one expects that, by increasing the intensity of the noise, $\hat{\rho}^{(0)}(t_q)$ will evolve into the statistical mixture of phase states $\sum_k \hat{\rho}^{(0)}_{kk}(t_q)$; moreover, the larger the atom number N the weaker should be the noise strength at which this occurs [39, 40]. It was found in [22] that for the phase noise considered in Sec.III the actual scenario for decoherence is different from the usual one. Indeed, the typical noise intensity at which the coherences between distinct phase states $|\pi/2, \phi_{k,q}\rangle$ are lost turns out to be independent of the atom number. This is a consequence of the fact that the decoherence factor $a(t)$ is independent of N, as shown in Sec.III B. Furthermore, for superpositions with a large number of components q, this intensity is *larger than* the noise intensity at which phase relaxation occurs. In what follows we discuss the origin of this fact.

Since the noise is expected to destroy correlations between different components, we decompose the density matrix in its diagonal (intra-component) and off-diagonal (intercomponent) parts, focussing on the latter one to quantify the decoherence. We have then $\hat{\rho}^{(0)} = \hat{\rho}^{(0)}_{\mathrm{d}} + \hat{\rho}^{(0)}_{\mathrm{od}}$ where

$$\hat{\rho}^{(0)}_{\mathrm{d}}(t_q) = \sum_{k=0}^{q-1} \hat{\rho}^{(0)}_{kk}(t_q) \quad (30)$$

and

$$\hat{\rho}^{(0)}_{\mathrm{od}}(t_q) = \sum_{k,k'=0;k\neq k'}^{q-1} \hat{\rho}^{(0)}_{kk'}(t_q). \quad (31)$$

Using Eq.(1) and the identity $\sum_{k=0}^{q-1} e^{2ik(n'-n)\pi/q} = q$ if $n = n'$ modulo q and 0 otherwise, the matrix elements of $\hat{\rho}^{(0)}_{\mathrm{d}}(t_q)$ in the Fock basis are

$$\langle n_z = n|\hat{\rho}^{(0)}_{\mathrm{d}}(t_q)|n_z = n'\rangle \quad (32)$$
$$= \begin{cases} \dfrac{(-1)^{2pI(\frac{N}{2})}}{2^N}\dbinom{N}{\frac{N}{2}+n}^{\frac{1}{2}}\dbinom{N}{\frac{N}{2}+n'}^{\frac{1}{2}} & \text{if } n' = n+pq \\ 0 & \text{if } n' \neq n \bmod q \end{cases}$$

where p is an integer and I denotes the integer part. By using $\hat{\rho}^{(0)}_{\mathrm{od}}(t_q) = e^{-i\pi\hat{J}_z^2/q}|\theta = \pi/2, \phi = 0\rangle\langle\theta = \pi/2, \phi = $

$0|e^{i\pi \hat{J}_z^2/q} - \hat{\rho}_{\mathrm{d}}^{(0)}(t_q))$, we also get

$$\langle n_z = n|\hat{\rho}_{\mathrm{od}}^{(0)}(t_q)|n_z = n'\rangle \qquad (33)$$

$$= \begin{cases} 0 & \text{if } n' = n + pq \\ \dfrac{e^{i\alpha_{nn'}}}{2^N}\dbinom{N}{\frac{N}{2}+n}^{\frac{1}{2}}\dbinom{N}{\frac{N}{2}+n'}^{\frac{1}{2}} & \text{if } n' \neq n \bmod q \end{cases}$$

with $\alpha_{nn'} = (n'+n-N)(n'-n)\pi/q$. The use of Eq.(27) allows to obtain the corresponding expressions in the presence of noise,

$$\langle n|\hat{\rho}_{\mathrm{d,od}}(t_q)|n'\rangle = e^{-\frac{a_q^2(n-n')^2}{2}}\langle n|\hat{\rho}_{\mathrm{d,od}}^{(0)}(t_q)|n'\rangle \qquad (34)$$

up to a phase factor irrelevant for decoherence, with $a_q \equiv a(t_q)$. In the strong noise limit $a_q \gg 1$, the off-diagonal part $\hat{\rho}_{\mathrm{od}}$ of the atom density matrix vanishes whereas the diagonal part $\hat{\rho}_{\mathrm{d}}$ tends to a matrix which is diagonal in the Fock basis,

$$\hat{\rho}_{\mathrm{d}}(t_q) \to \hat{\rho}_\infty = \int_0^{2\pi}\frac{d\phi}{2\pi}|\theta=\pi/2,\phi\rangle\langle\theta=\pi/2,\phi| \qquad (35)$$

$$= \sum_{n=-N/2}^{N/2}\frac{1}{2^N}\binom{N}{\frac{N}{2}+n}|n_z=n\rangle\langle n_z=n|.$$

The fact that the diagonal part of the atom density matrix decays faster than the off-diagonal part for increasing noise strengths [22] is readily explained by examining the structure of the noiseless density matrices in Eqs.(32) and (33). The first off-diagonal elements of $\hat{\rho}_{\mathrm{d}}(t_q)$ in the Fock basis are those for which $n' = n \pm q$ while the first off-diagonal elements of $\hat{\rho}_{\mathrm{od}}(t_q)$ satisfy $n' = n \pm 1$. Hence, it results from Eq.(34) that the off-diagonal elements of $\hat{\rho}_{\mathrm{d}}$ vanish at the noise scale $a \simeq 1/q$ while the off-diagonal elements of $\hat{\rho}_{\mathrm{od}}$ vanish at the larger noise scale $a \simeq 1$. In other words, the noise is more effective in letting $\hat{\rho}_{\mathrm{d}}$ converge to $\hat{\rho}_\infty$ than in suppressing $\hat{\rho}_{\mathrm{od}}$, and this effect is more pronounced the higher is the number of components in the superposition. An illustration of such anomalous decoherence is given in Fig. 2. The middle panels show that for intermediate noise strengths, $\hat{\rho}_{\mathrm{d}}$ has already acquired its asymptotic diagonal form (35), while $\hat{\rho}_{\mathrm{od}}$ has not yet vanished. As we will see in Sec.V B below, these results imply that, for moderate strengths of phase noise, macroscopic superpositions are formed and provide quantum correlations useful for interferometry.

B. Angular momentum distributions

The anomalous decoherence of the atomic state can be visualized by plotting the probability distribution $P_\phi(r)$ of the eigenvalues of the angular momentum operators $\hat{J}_\phi = \hat{J}_x\sin\phi - \hat{J}_y\cos\phi$ in an arbitrary direction of the equatorial plane of the Bloch sphere [41]. The presence of correlations among the components of the superposition formed at time t_q is indicated by interference fringes in
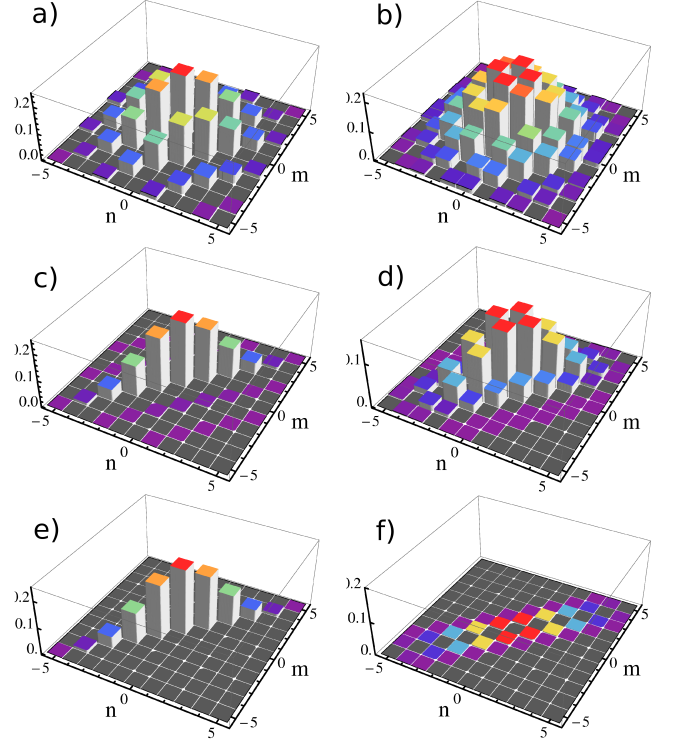

FIG. 2. (Color online) Matrix elements of the diagonal (intra-component) part $\hat{\rho}_{\mathrm{d}}(t_3)$ (panels a),c),e)) and the off-diagonal (inter-component) part $\hat{\rho}_{\mathrm{od}}(t_3)$ (panels b),d),f)) of the density matrix in the Fock basis at time $t = t_3$ as the noise is increased from $a_3 = 0$ (a),b)) to $a_3 = 0.9$ (c),d)) and $a_3 = 2.9$ (e),f)).

these distributions, which would be absent if the atoms would be in a statistical mixture of phase states.

The probability distribution of $\hat{J}_\phi$ in the state $\hat{\rho}$ can be calculated by a straightforward generalization of the calculation in [41], as the Fourier coefficient of the characteristic function $h_\phi(\eta) = \mathrm{tr}[e^{-i\eta\hat{J}_\phi}\hat{\rho}]$, namely,

$$P_\phi(r;t) = \frac{1}{2\pi}\int_{-\pi}^{\pi}d\eta\, h_\phi(\eta;t)e^{i\eta r}. \qquad (36)$$

For the quenched dynamics of the Bose Josephson junction in the presence of noise, the characteristic function reads

$$h_\phi(\eta;t) = \sum_{n,n'=-N/2}^{N/2}g_{nn'}(t)\langle n_z=n|\hat{\rho}^{(0)}(t)|n_z=n'\rangle$$
$$\times D_{n'n}(-\phi,\eta,\phi) \qquad (37)$$

where $g_{nn'}(t) = e^{-a^2(t)(n-n')^2/2}e^{i\overline{\lambda}t(n-n')}$ and $D_{n'n}(-\phi,\eta,\phi)$ is the matrix element of the rotation operator $e^{-i\eta J_\phi}$ in the Fock basis, which is given by
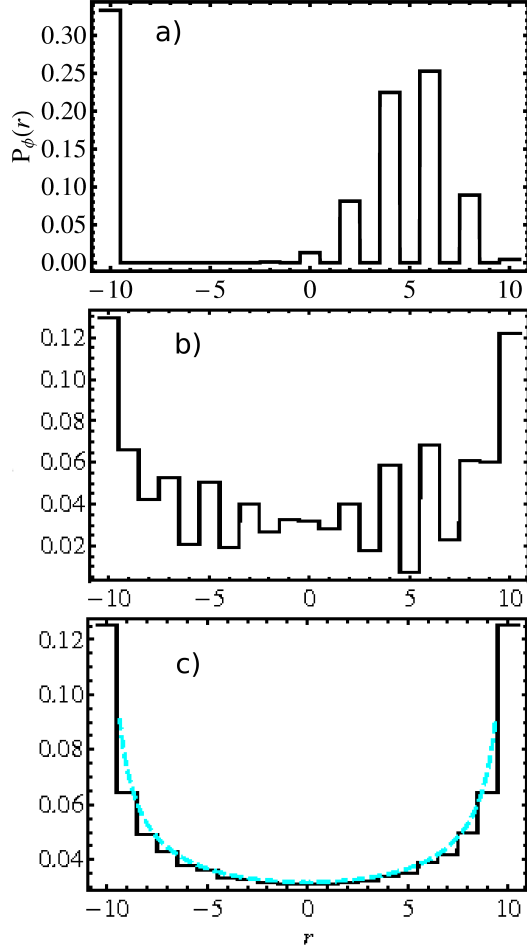
FIG. 3. (Color online) Probability distribution $P_{\pi/2}(r, t_3)$ of the eigenvalues of $\hat{J}_x$ for the three-component coherent superposition (solid lines) at increasing noise strength from $a_3 = 0$ (a),b)), to $a_3 = 0.9$ (c),d)) and $a_3 = 2.9$ (e),f)) with $N = 20$ atoms. The blue dashed curves indicate the large-noise intensity and large N limit given by Eq.(39).

(see e.g. [42], Eq. (D6))

$$D_{n'n}(-\phi, \eta, \phi) = \langle n_z = n' | e^{-i\eta J_\phi} | n_z = n \rangle$$

$$= \sum_{k=\max\{0,n-n'\}}^{\min\{N/2-n',N/2+n\}} (-1)^k \binom{N}{\frac{N}{2}+n}^{-\frac{1}{2}} \binom{N}{\frac{N}{2}+n'}^{-\frac{1}{2}}$$

$$\times \frac{N!}{(\frac{N}{2}-n'-k)!(\frac{N}{2}+n-k)!k!(k+n'-n)!} \quad (38)$$

$$\times \left(\sin\frac{\eta}{2}\right)^{2k+n'-n} \left(\cos\frac{\eta}{2}\right)^{N+n-n'-2k} e^{-i\phi(n'-n)}.$$

The probability distribution in the absence of noise derived in [41] is recovered by setting $g_{nn'}(t) = 1$ in Eq.(37).

The distribution $P_{\pi/2}(r, t_3) = |\langle n_x = r | \psi^{(0)}(t_3) \rangle|^2$ of the eigenvalues of $\hat{J}_x$ (satisfying $\hat{J}_x | n_x = r \rangle = r | n_x = r \rangle$) is shown in Fig.3 for the three-component superposition of phase states in the absence of noise (panel a)). Its pro-

file displays two peaks corresponding to the projections on the x-axis of the phase states $|\theta = \pi/2, \phi = \phi_{k,3}\rangle$, $\phi_{k,3} = 0, 2\pi/3, 4\pi/3$ (the "phase content" of the state, accounted for by $\hat{\rho}_d(t_3)$) and interference fringes, due to the coherences between these phase states (contained in $\hat{\rho}_{od}(t_3)$). In the presence of noise (b)-c)), the phase profile of each component of the superposition spreads and the characteristic peaks in the profile of the distribution are smeared out (phase relaxation). At strong noise intensities, $\hat{\rho}_d(t_q)$ approaches the steady-state given by the density matrix (35), which is symmetric in the (xOy)-plane. As a consequence, the corresponding probability distribution $P_\phi(r, \infty) \equiv P(r, \infty) = \text{tr}[\hat{\rho}_\infty | n_x = r \rangle \langle n_x = r |]$ is independent on ϕ. In the semi-classical limit $N \gg 1$, this distribution can be easily calculated since $\hat{J}_x$ takes the values $N \cos \phi/2$ in the phase states $|\pi/2, \phi\rangle$ apart from small relative fluctuations of the order of $1/\sqrt{N}$. Hence, recalling that $\hat{\rho}_\infty$ is a statistical mixture of the states $|\pi/2, \phi\rangle$ with equal probabilities (see Eq.(35)),

$$P(r, \infty) = c \int_0^{2\pi} d\phi \, \delta\left(\frac{N}{2}\cos\phi - r\right) = \frac{1}{\pi} \frac{1}{\sqrt{\left(\frac{N}{2}\right)^2 - r^2}}$$
$$(39)$$

where c is a normalization factor. The semi-circle law (39) is indicated by the blue dashed curve in panel c) of Fig.3. For finite N, one finds

$$P(r, \infty) = \binom{N}{\frac{N}{2}+r} \frac{1}{\pi} \frac{\Gamma\left[\frac{N}{2} + \frac{1}{2} - r\right] \Gamma\left[\frac{N}{2} + \frac{1}{2} + r\right]}{\Gamma[N+1]}.$$

On the other hand, the vanishing of $\hat{\rho}_{od}(t_q)$ tends to diminish the contrast of the fringes in the distribution $P_\phi(r, t_q)$, until they are completely washed out in the asymptotic distribution (panel c) of Fig.3). The fact that phase relaxation occurs at a lower noise strength than decoherence is evident in the panel b), where the profile of $P_\phi(r, t_q)$ is close to the asymptotic distribution $P(r, \infty)$ while interference fringes due to $\hat{\rho}_{od}(t_q)$ are still visible.

V. QUANTUM FISHER INFORMATION AND COHERENT SPIN SQUEEZING DURING THE QUENCHED DYNAMICS OF A BJJ

We present in this section the estimate of the useful quantum correlations which are formed during the quenched dynamics of the Bose Josephson junction introduced in Secs.III and IV. For this purpose, we evaluate the quantum Fisher information and the coherent spin squeezing parameter. We consider first the noiseless evolution for which analytical expressions can be obtained, then we present the numerical results for the dynamical evolution in the presence of noise.

A. Dynamics in the absence of noise

In the absence of noise the atoms are in a pure state $|\psi^{(0)}(t)\rangle$ during all the dynamical evolution. The co-

variance matrix $\gamma^{(0)}(t)$ associated to this state is thus given by Eq.(16). For the quenched dynamics described in Sec.III by using Eqs. (1), (18), one finds that

$$\langle \hat{J}_y \rangle_t^{(0)} = \langle \hat{J}_z(t) \rangle_t^{(0)} = 0, \qquad (40)$$

$$\langle \hat{J}_x \rangle_t^{(0)} = \frac{N}{2} \cos^{N-1}\left(\frac{2\pi t}{T}\right) \equiv \frac{N}{2} \nu^{(0)}(t), \qquad (41)$$

where $\langle .. \rangle_t^{(0)} = \mathrm{tr}(...\hat{\rho}^{(0)}(t))$ and $\nu^{(0)}(t)$ corresponds to the visibility of the Ramsey fringes [10]. The angular-momenta covariance matrix (16) finally reads

$$\gamma^{(0)}(\tau) = \begin{pmatrix} \gamma_x^{(0)}(\tau) & 0 & 0 \\ 0 & -\frac{N}{8}\left[(N-1)\cos^{N-2}(2\tau) - (N+1)\right] & \frac{N(N-1)}{4}\cos^{N-2}(\tau)\sin(\tau) \\ 0 & \frac{N(N-1)}{4}\cos^{N-2}(\tau)\sin(\tau) & \frac{N}{4} \end{pmatrix} \qquad (42)$$

where we have introduced the rescaled time $\tau = 2\pi t/T = \chi t$ and

$$\gamma_x^{(0)}(\tau) \equiv \langle (\Delta \hat{J}_x)^2 \rangle_\tau^{(0)} = \frac{N}{8}\left[(N-1)\cos^{N-2}(2\tau) + (N+1) - 2N\cos^{2(N-1)}(\tau)\right]. \qquad (43)$$

The two other eigenvalues of the matrix (42) are

$$\gamma_\pm^{(0)}(\tau) = \frac{N}{16}\left[-(N-1)\cos^{N-2}(2\tau) + (N+3) \pm (N-1)\sqrt{(\cos^{N-2}(2\tau) - 1)^2 + 16\cos^{2(N-2)}(\tau)\sin^2(\tau)}\right] \qquad (44)$$

(see also Ref.[43]). We remark that the matrix (42) has the property that its eigenvalues at times τ and $\pi - \tau$ (and, similarly, at $2\pi - \tau$) coincide, hence it suffices to discuss its behaviour at times t belonging to the interval $[0, T/4]$ (i.e., $\tau \in [0, \pi/2]$).

According to Eq.(15), the quantum Fisher information is given by the largest eigenvalue,

$$F_Q(\tau) = 4 \max\left\{\gamma_x^{(0)}(\tau), \gamma_+^{(0)}(\tau)\right\}. \qquad (45)$$

We demonstrate in Appendix C that the coherent spin squeezing (9) is always optimum along a direction contained in the (yOz)-plane. The optimal spin squeezing parameter (13) is thus related to the lowest eigenvalue $\gamma_-^{(0)}(\tau)$ of the submatrix $\gamma^{(0)}{}'(\tau)$ obtained by removing the first lign and column in the matrix (42). Using Eqs.(40) and (41), one gets

$$\xi^{(0)^2}(\tau) = \frac{4\gamma_-^{(0)}(\tau)}{N\nu^{(0)^2}(\tau)} \qquad (46)$$

The direction of optimum squeezing is given by the eigenvector

$$\vec{n}_\xi^{(0)}(\tau) = \vec{n}_-^{(0)}(\tau) = -\sin\theta_\xi^{(0)}(\tau)\, \vec{e}_y + \cos\theta_\xi^{(0)}(\tau)\, \vec{e}_z \qquad (47)$$

associated to the eigenvalue $\gamma_-^{(0)}(\tau)$ of the covariant matrix. One easily finds

$$\theta_\xi^{(0)}(\tau) = \arctan\left(\frac{\gamma_{yz}^{(0)}(\tau)}{\gamma_+^{(0)}(\tau) - \gamma_{zz}^{(0)}(\tau)}\right)$$
$$= \frac{1}{2}\arctan\left(\frac{\langle \{\hat{J}_y, \hat{J}_z\} \rangle_\tau^{(0)}}{\langle \hat{J}_y^2 \rangle_\tau^{(0)} - \langle \hat{J}_z^2 \rangle_\tau^{(0)}}\right) \qquad (48)$$

where $\{\cdot, \cdot\}$ denotes the anticommutator.

The direction of optimization $\vec{n}_F^{(0)}$ of the quantum Fisher information is either given by $\vec{e}_x$ (if $\gamma_x^{(0)} > \gamma_+^{(0)}$) or by the eigenvector $\vec{n}_+^{(0)}$ associated to the eigenvalue $\gamma_+^{(0)}$ (if $\gamma_x^{(0)} < \gamma_+^{(0)}$). The latter condition is satisfied at times shorter than t^*, see Appendix D. As both these eigenvectors are orthogonal to $\vec{n}_-^{(0)}$ (since the matrix $\gamma^{(0)}$ is symmetric), it follows that coherent spin squeezing and quantum Fisher information are optimized in perpendicular directions. At short times, when the state of the system is a squeezed state, this has a clear physical interpretation: the quantum Fisher information is maximum in the direction of maximal angular momentum fluctuations, which is perpendicular to the direction of lowest fluctuations yielding the best squeezing.

The Fisher information (45) and the squeezing parameter (46) obtained from Eqs.(43) and (44) are shown as a function of time in Fig. 4. At short times, the coherent spin squeezing (a)) is below one, indicating the presence of a squeezed state. To compare spin squeezing and Fisher information, we introduce the parameter
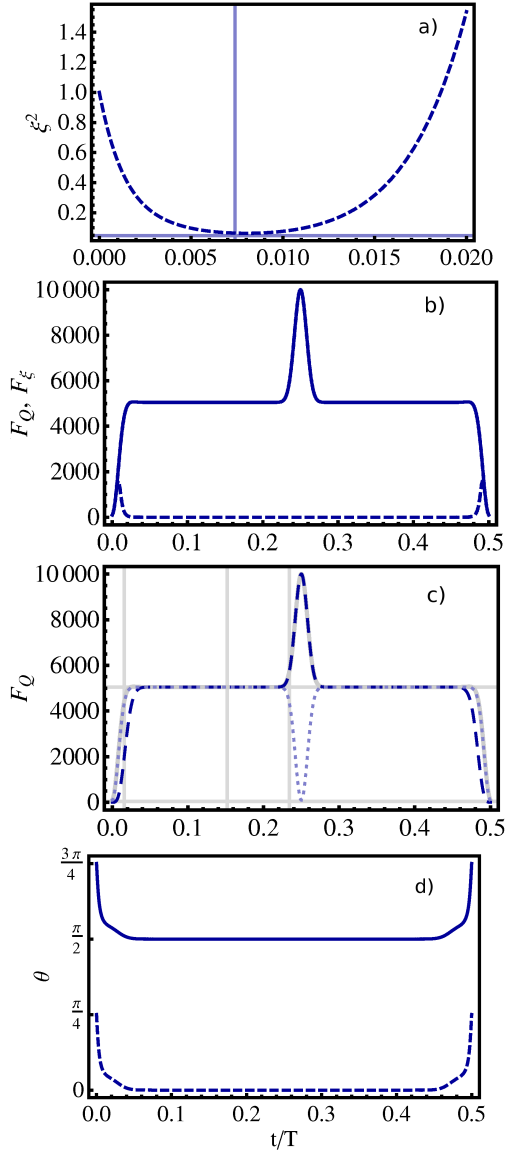
FIG. 4. (Color online) a) Coherent spin squeezing and b) quantum Fisher information during the quenched dynamics of a BJJ with $N = 100$ atoms as a function of time (in units of the revival time T) in the absence of noise. The dashed line in the second panel represents the parameter $F_\xi = N/\xi^2$. Horizontal and vertical gridlines in panel a): minimum of the coherent spin squeezing and corresponding time t_{min} (see text). c) Non-optimized quantum Fisher information along the x-axis (dashed line) and the y-axis (dotted line). For comparison, the optimum quantum Fisher information of panel b) is also shown (gray solid line). The vertical gridlines correspond from right to left to the time $t = t_{fs}$ of formation of the first macroscopic superposition, see Eq.(49); to $t = t^*$, see Appendix D; and to $t = T/4 - t_{fs}$. The horizontal gridline shows the shot-noise level $F_Q = N$. d) Angles $\theta_\xi^{(0)}$ in Eq.(48) (dashed line) and $\theta_F^{(0)}$ (solid line) giving the optimizing direction for the spin squeezing and the quantum Fisher information as a function of time.

$F_\xi = N/\xi^2$. This parameter was shown in [11] to coincide at short times with the Fisher information, indicating that F_Q and ξ provide essentially the same information for squeezed states at such times. This property is illustrated in Fig.4-b), and is demonstrated in the large N limit in Appendix E. At larger times, the squeezing parameter first reaches a minimum and then grows to values larger than one (that is, F_ξ decreases and becomes smaller than N). This does not imply that the atomic state is not useful for interferometry since, as described in Sec.II, the squeezing criterion is only a sufficient condition for useful entanglement [11]. Indeed, the quantum Fisher information increases above the shot noise level $F_Q = N$ until it reaches a plateau value $F_Q \simeq N(N+1)/2$ (see Appendix E), at the time

$$t_{fs} \sim T/\sqrt{N}. \tag{49}$$

This time corresponds to the time of formation of the "first" (in chronological order) multicomponent superposition, as one can infer from the following argument. The largest number of phase states of size $\sqrt{N}/2$ (see Sec.II A) which can be put on the equator of the Bloch sphere of radius $N/2$ is $q_{max} \simeq 2\pi N/\sqrt{N} = 2\pi\sqrt{N}$. The time of formation of the multicomponent superposition with the highest number of phase states is $t_{fs} = T/(2q_{max})$, leading to Eq. (49). Note that t_{fs} is also the time scale for phase diffusion, that is, for the decay of the visibility (41). It is seen in Fig.4 that F_Q displays a sharp maximum at $t = t_2 = T/4$, in correspondence to the two-component macroscopic superposition which has the highest possible Fisher information $F_Q = N^2$. This result is not surprising since this two-component superposition (19) is the analog in the phase variable of a NOON state, from which it can be obtained by a $\pi/2$ rotation around the y-axis. Panel c) of Fig.4 shows the Fisher information in the directions $\vec{e}_x$ and $\vec{e}_y$. In the time regime corresponding to the plateau, they are almost equal due to the symmetry of the multicomponent superpositions (this means that the eigenvalues $\gamma_x^{(0)}$ and $\gamma_+^{(0)}$ are almost degenerate). As one approaches the two-component superposition, the optimizing direction changes to the x-axis, which is the direction of maximal angular momentum fluctuations.

In panel d) of Fig.4, the angle $\theta_\xi^{(0)}$ giving the direction of highest spin squeezing in the (yOz) plane is represented as a function of time together with the corresponding angle $\theta_F^{(0)}$ for the Fisher information, which gives the optimizing direction $\vec{n}_F^{(0)}$ of the Fisher information according to Eq.(11). Table II summarizes the aforementioned results. Some analytical results obtained for short, intermediate and long times in the limit $N \gg 1$ of a large number of atoms are given in AppendixE.

Time	Optimum quantum Fisher information F_Q	Optimizing direction
$t = 0$	N	degenerate in (yOz) plane
$0 \leq t \lesssim T/N$	$\nearrow$, given by Eq.(E1)	$-\cos\theta_\xi^{(0)}(t)\,\vec{e}_y - \sin\theta_\xi^{(0)}(t)\,\vec{e}_z$
$T/N \ll t \leq t_{\min}$	$\nearrow$, given by Eq.(E1)	$\simeq \vec{e}_y$
$t_{\min} < t \lesssim t_{fs}$	$\nearrow$, $3^{1/3}N^{5/3} < F_Q \lesssim 0.4323N^2$	$\simeq \vec{e}_y$
$t_{fs} \ll t \leq t^*$	$\longrightarrow$, $F_Q \simeq N(N+1)/2$	$\simeq \vec{e}_y$
$t^* < t \leq T/4$	$\nearrow$, $N(N+1)/2 \lesssim F_Q \leq F_Q(T/4) = N^2$	$\vec{e}_x$ if N is even, $\simeq \vec{e}_y$ if N is odd
Time	Optimum coherent spin squeezing parameter $F_\xi \equiv N/\xi^2$	Optimizing direction
$t = 0$	N	degenerate in (yOz) plane
$0 \leq t \lesssim T/N$	$\nearrow$, $F_\xi \simeq F_Q$	$-\sin\theta_\xi^{(0)}(t)\,\vec{e}_y + \cos\theta_\xi^{(0)}(t)\,\vec{e}_z$
$T/N \ll t \leq t_{\min}$	$\nearrow$, $N < F_\xi \leq F_\xi(t_{\min}) = 2N^{5/3}3^{-2/3}$	$\simeq \vec{e}_z$
$t_{\min} < t \lesssim t_{fs}$	$\searrow$, $Ne^{-1/2} \lesssim F_\xi < 2N^{5/3}3^{-2/3}$	$\simeq \vec{e}_z$
$t_{fs} \ll t \leq t^*$	$\searrow$, $N/3^{N/2-1} \leq F_\xi \ll N$	$\simeq \vec{e}_z$
$t^* < t \leq T/4$	$\searrow$, $0 < F_\xi < N/3^{N/2-1}$	$\simeq \vec{e}_z$

TABLE II. Optimum coherent spin squeezing parameter, optimum quantum Fisher information and corresponding optimizing directions during the quenched dynamics of a Bose Josephson junction in the absence of noise for $N \gg 1$. The arrows indicate whether the function is increasing or decreasing with time in a given time interval.

B. Dynamics in the presence of noise

Let us now consider the effect of the phase noise introduced in Sec.III B on the results obtained in the previous subsection. For coherent spin squeezing the calculation can be carried out analytically. We start with the observation that even in the presence of noise $\langle\hat{J}_y\rangle_t = \langle\hat{J}_z\rangle_t = 0$ and more generally the angular-momentum covariance matrix G defined in Eq.(16) has the same structure as the matrix (42) in the noiseless case. Therefore, the arguments used in Appendix C can be taken over to the noiseful case. We thus conclude that the squeezing parameter ξ^2 is minimum in the (yOz)-plane, and is given by Eq.(46), evaluated for the corresponding quantities in the presence of noise. In particular, the bare visibility $\nu^{(0)}$, Eq.(41), should be replaced by the visibility ν in the presence of noise [22],

$$\nu(t) = \frac{2}{N}\langle\hat{J}_x\rangle_t = e^{-a^2(t)/2}\nu^{(0)}(t)\,, \tag{50}$$

and $\gamma_-^{(0)}$ by the lowest eigenvalue G_- of the restriction of the covariance matrix G to the (yOz)-plane.

We are now going to compute G_- and the spin squeezing parameter explicitly. In order to do so, we need to perform the averages in the presence of noise using the full density matrix $\hat{\rho}(t)$: $\langle\ldots\rangle_t = \mathrm{tr}(\ldots\hat{\rho}(t))$. They are related to those in the absence of noise according to

$$\langle\hat{J}_i\rangle_t = \int_{-\infty}^{\infty} d\phi\, f(\phi,t)\langle e^{i\phi\hat{J}_z}\hat{J}_i e^{-i\phi\hat{J}_z}\rangle_t^{(0)} \tag{51}$$

where the expectation value inside the integral is taken for the pure state $|\psi^{(0)}(t)\rangle$ in the absence of noise. The rotated angular momentum operators in the above expectation value are equal to $\cos\phi\hat{J}_x - \sin\phi\hat{J}_y$, $\sin\phi\hat{J}_x + \cos\phi\hat{J}_y$, and $\hat{J}_z$ for $i = x, y$, and z, respectively. A similar derivation holds for $\langle\{\hat{J}_i, \hat{J}_j\}\rangle_t = \mathrm{tr}[\hat{\rho}(t)\{\hat{J}_i, \hat{J}_j\}]$, with the result

$$\langle\hat{J}_z^2\rangle_t = \langle\hat{J}_z^2\rangle_t^{(0)} = \frac{N}{4}$$

$$\langle\hat{J}_y^2\rangle_t = \frac{1 - e^{-2a^2(t)}}{2}\langle\hat{J}_x^2\rangle_t^{(0)} + \frac{1 + e^{-2a^2(t)}}{2}\langle\hat{J}_y^2\rangle_t$$

$$\langle\{\hat{J}_y, \hat{J}_z\}\rangle_t = e^{-a^2(t)/2}\langle\{\hat{J}_y, \hat{J}_z\}\rangle_t^{(0)}$$

$$\langle\{\hat{J}_x, \hat{J}_y\}\rangle_t = \langle\{\hat{J}_x, \hat{J}_z\}\rangle_t = 0\,. \tag{52}$$

Finally, the submatrix matrix $G'(t)$ reads

$$G'(\tau) = \begin{pmatrix} \frac{N}{8}\left[-e^{-2a^2(\tau)}(N-1)\cos^{N-2}(2\tau) + (N+1)\right] & \frac{1}{4}e^{-\frac{a^2(\tau)}{2}}N(N-1)\cos^{N-2}(\tau)\sin(\tau) \\ \frac{1}{4}e^{-\frac{a^2(\tau)}{2}}N(N-1)\cos^{N-2}(\tau)\sin(\tau) & \frac{N}{4} \end{pmatrix}\,. \tag{53}$$

Thus, by Eqs.(46), (50) and (53), one has

$$\xi^2(\tau) = \frac{1}{4\nu^{(0)^2}(\tau)} \left[-e^{-a^2(\tau)}(N-1)\cos^{N-2}(2\tau) + e^{a^2(\tau)}(N+3) \right.$$

$$\left. -(N-1)e^{a^2(\tau)}\sqrt{(1-e^{-2a^2(\tau)}\cos^{N-2}(2\tau))^2 + 16e^{-a^2(\tau)}\cos^{2(N-2)}(\tau)\sin^2(\tau)} \right]. \qquad (54)$$

The angle which identifies the optimal squeezing direction is given by Eq.(48), in which the matrix $\gamma^{(0)}$ should be replaced by G'.

We proceed by illustrating our results for the squeezing parameter in the presence of phase noise. For the calculations we have chosen a noise range of direct experimental relevance, as extracted from the fit of the visibility decay data in Fig.4.15 of Ref. [35] with our prediction given by Eq.(50). For the noise variance $a^2(\tau)$ we take the short-time behavior $a^2(\tau) = (\delta\lambda/\chi)^2\tau^2$ expressed by Eq.(28) since the experimental visibility exhibits a gaussian decay even for small interactions χ [35]. This indicates that in the time regime $0 \leq t \lesssim t_{fs}$, the phase noise in the experiments has strong time correlations (colored noise). The squeezing parameter as a function of time is shown in Fig.5-a). As seen in the figure, the presence of noise degrades the squeezing, as its minimum value increases at increasing noise strength. We also notice that the time for optimal squeezing $t_{\min}$ is slighly shorter than in the noiseless case. As is shown in Appendix E in the limit of a large number of atoms we find that the minimum value of $\xi^2(\tau)$ is

$$\xi^2_{\min} \simeq (\xi^{(0)}_{\min})^2 + N^{-1}(\delta\lambda/\chi)^2 \qquad (55)$$

this minimum being reached to leading order at the same time $\tau_{\min} = \tau^{(0)}_{\min} = 3^{1/6}N^{-2/3}$ as in the noiseless case. This means that by increasing the number of atoms the noise becomes less efficient in limiting the highest squeezing which can be reached during the dynamical evolution. This results from the fact that the time $t_{\min}$ at which this highest squeezing is produced is shorter for larger N, whereas the effect of the noise on the density matrix (27) is independent of N, as stressed in Sec.III B. The angle $\theta_\xi(t)$ which identifies the optimizing squeezing direction is represented in dashed lines at various noise levels in Fig.5-d). As discussed in Appendix E, similar to the noiseless case, θ_ξ almost vanishes at intermediate times $N^{-1} \ll \tau \ll \pi/2 - N^{-1}$.

The evaluation of the optimum quantum Fisher information (14) requires a numerical diagonalization of the density matrix $\hat{\rho}(t)$ given by Eq.(27). For the time dependence of $a^2(t)$ we take again the short-time approximation given in Eq.(28), even if there is no experimental evidence which justifies such a choice at times $t \sim T$. This choice corresponds to the worst possible scenario for decoherence, as in the markovian regime the dependence of $a^2(t)$ is weaker (see Eq.(29)) [22]. The behaviour of F_Q as a function of time in the presence of noise results from the competition of two phenomena: (i) in the absence of noise, at short times the quantum Fisher information grows from its initial value $F_Q = N$ to the plateau value $F_Q = N(N+1)/2$ in a time interval $t_{fs} \sim T/\sqrt{N}$ which shrinks as N becomes larger, and (ii) the decoherence exponent $a^2(t)$ is independent of N and also grows with time. As a result, F_Q reaches a local maximum at a time $t_{\max} \sim t_{sf}$, with a value which increases with N and decreases with the noise fluctuation $\delta\lambda^2$.

The quantum Fisher information as a function of time at various noise levels is shown in Fig. 5. The short-time evolution is similar to the one found for the noiseless case, the accumulation of noise correlations being not yet effective. In particular, one observes that F_Q coincides with the squeezing parameter $F_\xi = N/\xi^2$ at sufficiently small times (panel c). For not too large noise intensities, F_Q displays a plateau at those times which in the noiseless BJJ correspond to the of formation of macroscopic superpositions. The value on the plateau is smaller than in the absence of noise but it is still much above the shot noise level $F_Q = N$. This indicates the presence of useful correlations which remain in spite of the decoherence effects induced by the noise. This effect is due to the robustness of the multicomponent superpositions [22] with respect to phase noise discussed in Sec. IV above. For higher noise levels, the width of the plateau is reduced and the peak at $t_2 \equiv T/4$ corresponding to the two-component superposition in the absence of noise disappears completely, meaning that decoherence has washed out the useful quantum correlations at t_2 (three bottom curves in the Fig.5-b)). In the limit of very large noise intensities the Fisher information at times t_q of formation of q-component superpositions in the noiseless BJJ is degenerate in the (xOy) plane and tends to the asympototic value

$$F_Q[\hat{\rho}_\infty] = \frac{N(N-1)}{2N+2}, \qquad (56)$$

which can be readily obtained from Eqs.(15) and (35). As illustrated in Fig.6, apart from short times and around the peak at t_2, the optimization direction is in the (xOy)-plane and F_Q is almost degenerate in all directions of this plane, as in the noiseless case.

As a partial summary, the analysis of the time evolution of the quantum Fisher information indicates the build-up of useful quantum correlations at times beyond the spin-squeezing regime. In the following we quantify this effect by studying the dependence of F_Q with the noise strength and the particle number.

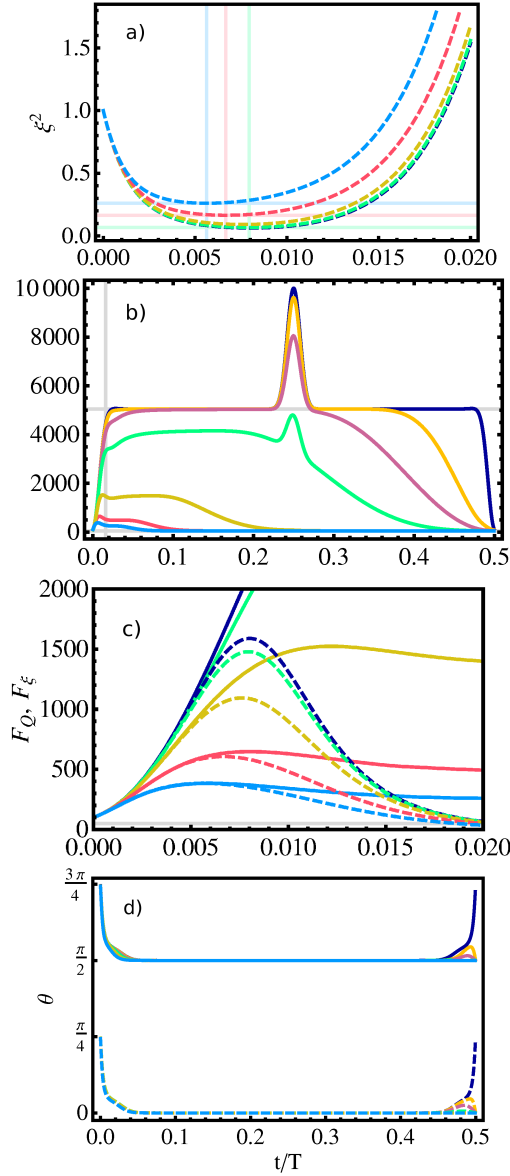Figure 7 shows $F_Q(t)$ on a logarithmic scale, evalu-

FIG. 5. (Color online) Coherent spin squeezing and quantum Fisher information in the presence of noise as a function of time in units of T during the quenched dynamics of a BJJ. The parameters used are $N = 100$, $\chi = \pi$ Hz. a) Spin squeezing ξ^2 for (from top to bottom) $\delta\lambda = 15, 10, 5,$ and 0 Hz. Horizontal and vertical gridlines: minimum of ξ^2 and corresponding time $t_{\min}$. b) Fisher information F_Q for (from top to bottom) $\delta\lambda = 0, 0.4, 1, 2, 5, 10,$ and 15 Hz; the horizontal and vertical gridlines correspond to $F_Q = N(N+1)/2$ and $t = t_{fs} = T/\sqrt{N}$. c) Zoom on the quantum Fisher information (solid lines) and $F_\xi = N/\xi^2$ (dashed lines) for $\delta\lambda = 0, 2, 5, 10,$ and 15 Hz (from top to bottom). d) Angles θ_F and θ_ξ giving the optimizing direction of F_Q (solid lines) and ξ^2 (dashed lines) as a function t/T, for the same noise levels.
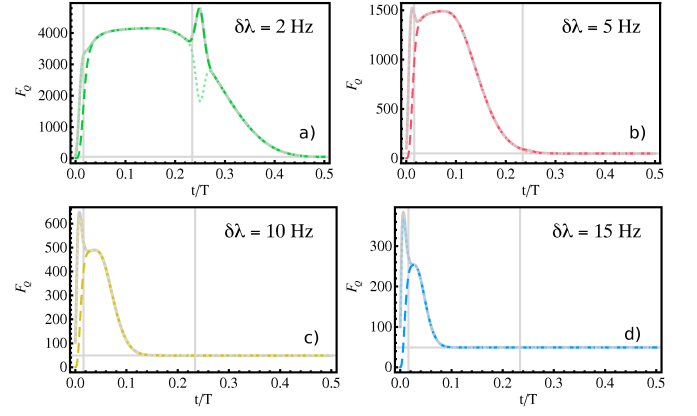

FIG. 6. (Color online) Direction-dependent quantum Fisher information in the presence of noise as a function of time in units of T during the quenched dynamics of a BJJ with $N = 100$ atoms and $\chi = \pi$Hz for: a) $\delta\lambda = 2$Hz, b) 5Hz, c) 10Hz and d) 15Hz, calculated along the (Ox) direction (dashed lines), the (Oy) direction (dotted lines) and the optimizing direction (light-gray solid line). After a time $t \sim T/\sqrt{N}$ (left vertical gridlines) the three values are almost the same, showing that the Fisher information is almost degenerate in the (xOy) plane, except around $t = T/4$ if F_Q has a peak at this value (panel a)). The vertical and horizontal gridlines represent the times $t = t_{fs}$ and $t = T/4 - t_{fs}$ and the value of the Fisher information in the limit of large noise intensities given by Eq.(56).
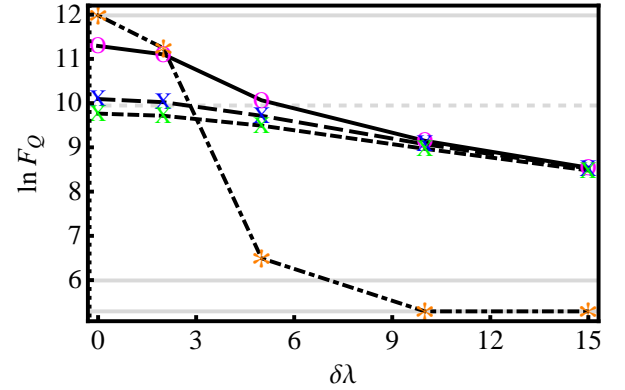

FIG. 7. (Color online) Values of the Fisher information at its local maximum at time $t_{\max}$ (solid line, circle markers), at time t_2 (dot-dashed line, star markers) and at the time $t_{\min}$ of maximal squeezing (long-dashed line, blue cross markers) in a logarithmic scale, as a function of the energy fluctuation $\delta\lambda$ (in Hz). For comparison we also plot the squeezing parameter $F_\xi = N/\xi^2$ at the time $t_{\min}$ (dashed line, green cross markers) in a logarithmic scale. Gridlines, from top to bottom: Heisenberg limit N^2 (solid), approximate value $(2/3^{2/3})N^{5/3}$ of $F_\xi(t_{\min})$ in the absence of noise, see Sec.V A (dashed), shot noise limit (solid), and limit of F_Q for large noise intensities (solid) given by Eq.(56). The parameters used are $N = 400$ and $\chi = \pi$ Hz.

ated at the time $t = t_2 \equiv T/4$ of formation of the two-component superposition in the noiseless BJJ, as well as the maximum $(F_Q)_{\max}$ of $F_Q(t)$ in the time interval $0 < t < T/8$. This maximum corresponds roughly to the value at the plateau in Fig.5, that is, to the value of $F_Q(t)$ at the times of formation of the first multicomponent superpositions. It can be seen that in the range of noise considered $(F_Q)_{\max}$ stays above the shot noise level, and is also larger than the value $F_Q(t_{\min})$ at the time $t_{\min}$ of highest squeezing. The two-component superposition, formed much after the superpositions with a large number of components, appears to be too much degraded by noise to lead to any advantage in interferometry with respect to separable states. Hence, in this regime multicomponent macroscopic superpositions provide a convenient alternative to both the squeezed states and the two-component macroscopic superposition.

We next study the scaling of the quantum Fisher information with the particle number, taken at the time $t_{\max}$ as before. As it is illustrated in Fig.8, at such a time F_Q displays a power-law behaviour $F_Q \sim N^\beta$ with an exponent β depending on the noise strength. This exponent is extracted from a log-linear fit of the numerical data, varying N between 50 and 400 [44], the latter value being realistic in the experiments [6]. We notice that in the noise range considered β is larger or equal to $5/3$, which is the exponent corresponding to the squeezed state at $t = t_{\min}$ in the absence of noise (see Sec.V A) [45]. This confirms the potential improvement in interferometry given by the state at time $t_{\max}$ with respect to the use of squeezeed states in the presence of phase noise. For comparison, we also show the scaling of F_Q at the time t_2. At that time, β decays faster with the noise strength, reaching rapidly the shot noise limit $\beta = 1$. This is due to the fact that the noise exponent $a^2(t)$ increases with time.

VI. CONCLUSIONS

In this work we have studied the effect of phase noise on the formation of nonclassical states useful for interferometry created during the quenched dynamics of a Bose Josephson junction. The knowledge of an exact solution for the dynamical evolution of the state in the presence of phase noise has allowed us to calculate the quantum Fisher information as a function of time and its scaling with the particle number at various noise strengths. Due to the anomalously slow decoherence induced by phase noise on macroscopic superpositions of phase states, for a realistic choice of noise strengths we have found that multicomponent superpositions are more useful for interferometry than squeezed states. Such superpositions are built during the dynamical evolution of a noiseless junction at larger times than squeezed states. The time of formation of the superposition with $\sim \sqrt{N}$ components depends inversely on the square-root of the total number of atoms N. When phase noise is affecting the unitary
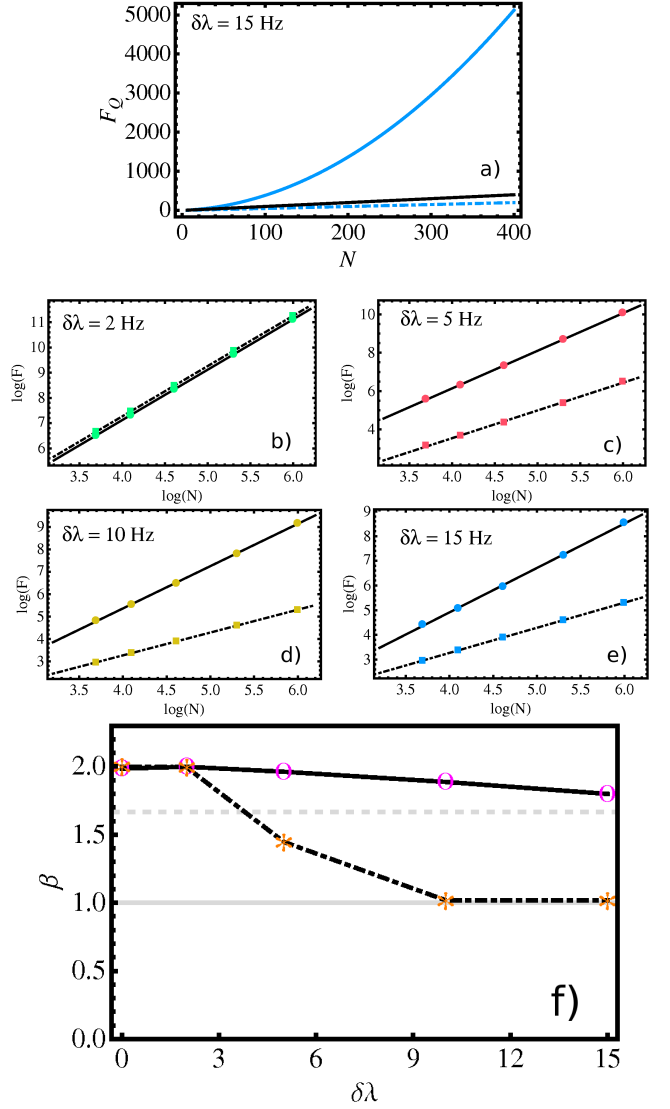

FIG. 8. (Color online) a) Quantum Fisher information evaluated at the time of its local maximum $t_{\max}$ (blue solid line) and at the time t_2 (blue dashed line) as a function of the number of particles N for $\delta\lambda = 15$ Hz, as compared to the shot noise limit (black solid line). Panels b),c),d),e): same as in a) in a semi-logarithmic scale, for various noise strengths $\delta\lambda = 2, 5, 10,$ and 15 Hz (from left to right and top to bottom). f) Exponent β, extracted by a log-linear fit of the data in a), as a function of the energy fluctuations $\delta\lambda$ (in Hz) for $t = t_{\max}$ (solid line, circle markers) and for $t = t_2$ (dot-dashed line, star markers). We used $\chi = \pi$ Hz.

dynamics of the junction, these multicomponent superpositions therefore provide an interesting alternative to the use of the more popular two-component superposition, which would appear later in a noiseless junction.

Appendix A: Derivation of the probability distribution $f(\phi, t)$ for gaussian noise

The probability distribution $f(\phi, t)$ of the angle $\phi(t) = -\int_0^t d\tau \lambda(\tau)$ is defined as an average over the noise realizations induced by the functional $P[\lambda(t)]$ as in Eq.(22), or, by Fourier expansion,

$$f(\phi, t) = \frac{1}{2\pi} \int dP\left[\lambda(t)\right] \int_{-\infty}^{\infty} du\, e^{-iu\phi(t)} e^{i\phi u} . \quad (A1)$$

We are left to evaluate the Fourier transform of the average $\overline{e^{-iu\phi(t)}} = \int dP[\lambda(t)] e^{-iu\phi(t)}$. This is readily done under the hypotesis of a gaussian noise,

$$
\begin{aligned}
\overline{e^{-iu\phi(t)}} &= \overline{e^{-iu(\phi(t)-\overline{\phi(t)})}} e^{-iu\overline{\phi(t)}} \\
&= e^{-\frac{u^2}{2}\overline{(\phi(t)-\overline{\phi(t)})2}} e^{-iu\overline{\phi(t)}} \\
&= e^{-\frac{u^2}{2}\int_0^t d\tau \int_0^t d\tau' h(\tau-\tau')} e^{-iu\overline{\lambda}t} \\
&= e^{-\frac{u^2}{2}a^2(t)} e^{-iu\overline{\lambda}t}
\end{aligned}
\quad (A2)
$$

where $h(\tau - \tau') = \overline{\lambda(\tau)\lambda(\tau')} - \overline{\lambda(0)}^2$ is the noise correlation function and we used that for gaussian variables with $\overline{\xi} = 0$ one has $\overline{e^{iu\xi}} = e^{-\frac{u^2}{2}\overline{\xi^2}}$. Using Eq.(A2) we obtain the expression (24) in the main text, according to

$$f(\phi, t) = \frac{1}{2\pi} \int_{-\infty}^{\infty} du\, e^{-i(\phi+\overline{\lambda}t)u} e^{-\frac{u^2}{2}a^2(t)} . \quad (A3)$$

Appendix B: Partial suppression of phase noise by spin-echo pulses

In a recent experiment [6], phase noise was partially suppressed by a spin-echo protocol [36]. Let us assume that the state of interest (for instance, a squeezed state in [6]) is produced after an evolution time t under the Hamiltonian (20). In the spin-echo protocol, two short π-pulses are send by a laser in resonance with the energies of the two modes at times $t/2$ and t. The effect of these laser pulses is to reverse the direction of $\hat{J}_z$, mapped into $-\hat{J}_z$, in the evolution between $t/2$ and t. Since the noiseless part of the Hamiltonian (20) is quadratic in $\hat{J}_z$, it is not affected by the pulses, while the noise part is linear in $\hat{J}_z$ and is reversed after half of the evolution. This allows to suppress the effect of the noise if it is strongly correlated between the two time intervals $[0, t/2]$ and $[t/2, t]$, which appears to be the case in the experiment of Ref.[6] (see also [35]).

Our model in Sec.III B can be easily adapted to take into account the residual effect of phase noise when the spin-echo pulses are applied. The derivation follows the same lines as in the main text. Eq.(27) still holds provided that we use $\phi(t) \equiv \int_0^t d\tau\, \mathrm{Sgn}(\tau - t/2)\lambda(\tau)$, with the sign function defined as $\mathrm{Sgn}(x) = \pm 1$ for $\pm x > 0$. This leads to

$$a_{\mathrm{echo}}^2(t) = \int_0^t d\tau \int_0^t d\tau'\, \mathrm{Sgn}(\tau - \frac{t}{2})\mathrm{Sgn}(\tau' - \frac{t}{2})h(\tau - \tau'). \quad (B1)$$

We focus on the short time regime $t < t_c$. The approximation $h(\tau) \simeq h(0)$ yields no contribution to $a_{\mathrm{echo}}^2(t)$. An expansion to second order is needed, $h(\tau) = h(0) + \tau h'(0) + \tau^2 h''(0)/2 + O(\tau^3)$. Using the parity $h(-\tau) = h(\tau)$ of the correlation function (which implies $h'(0) = 0$), we obtain [47]

$$a_{\mathrm{echo}}^2(t) = -\frac{h''(0)}{16} t^4 . \quad (B2)$$

Comparing Eqs. (B2) and (28), one sees that the effect of the noise at times $t < t_c$ is considerably reduced with respect to the case in absence of spin echo.

Appendix C: Demonstration of Eq.(46) for the spin squeezing parameter

In the following we show that the spin squeezing parameter $\xi^2(t)$ in a Bose Josephson junction is always optimized along a direction contained in the (yOz)-plane.

Let us observe that the angular momentum covariance matrix $G(t)$ defined by Eq.(16) has vanishing matrix elements $G_{xy}(t) = G_{xz}(t) = 0$. In fact, in the absence of noise this matrix $G(t) = \gamma^{(0)}(t)$ is given by Eq.(42), and we have seen in Sec. V B that it preserves the same structure in the presence of a phase noise. Thanks to this special structure of $G(t)$, the fluctuations of the angular momentum operator along an arbitrary direction $\vec{n}$ given by Eq.(11) is

$$
\begin{aligned}
\Delta J_{\vec{n}}(t) &= \sum_{i,j=x,y,z} n_i G_{ij}(t) n_j \quad (C1) \\
&= \sin^2\theta \sin^2\phi\, G_{xx}(t) + \sum_{i,j=y,z} n_i G_{ij}(t) n_j .
\end{aligned}
$$

The sum over i, j in the second line can be written as $(\sin^2\theta\cos^2\phi + \cos^2\theta)\vec{n}'^T G'(t)\vec{n}'$, where we introduced the notation $G'(t)$ for the two-by-two submatrix of $G(t)$ in the plane (yOz) and the normalized vector

$$\vec{n}' = \frac{n_y \vec{e}_y + n_z \vec{e}_z}{\sqrt{\sin^2\theta\cos^2\phi + \cos^2\theta}} \quad (C2)$$

in this plane. Furthermore, we observe that during the dynamics of the noisy junction one has $\langle \hat{J}_y \rangle_t = \langle \hat{J}_z \rangle_t = 0$ at all times. As a consequence, the expectation values

of the angular momentum operators along the directions defined by Eq.(10) are given by

$$\langle \hat{J}_{\vec{p}_1} \rangle_t = \cos\phi \langle \hat{J}_x \rangle_t$$
$$\langle \hat{J}_{\vec{p}_2} \rangle_t = -\cos\theta \sin\phi \langle \hat{J}_x \rangle_t. \qquad (C3)$$

Combining these results and using the fact that $G_{xx}(t) \geq 0$, we obtain from Eq.(9)

$$\frac{N\nu(t)^2}{4}\xi_{\vec{n}}^2(t) = \frac{\sin^2\theta \sin^2\phi \, G_{xx}(t)}{1-\sin^2\phi\sin^2\theta} + \vec{n}'^T G'(t)\vec{n}'$$
$$\geq G_-(t) = \min_{\vec{n}',\|\vec{n}'\|=1}\left\{\vec{n}'^T G'(t)\vec{n}'\right\} \qquad (C4)$$
$$= \min_{\vec{n}\in(yOz),\|\vec{n}\|=1}\left\{\vec{n}^T G(t)\vec{n}\right\}$$

where $\nu(t) = 2\langle \hat{J}_x \rangle_t/N$ is the visibility and $G_-(t)$ the smallest eigenvalue of $G'(t)$. Since it is clear that the inequality in Eq.(C4) is an equality for $\vec{n}$ equal to the corresponding eigenvector $\vec{n}_-(t)$ of $G_-(t)$, this demonstrates that the squeezing is minimized along a direction $\vec{n}_-(t)$ contained in the (yOz)-plane. Combining Eqs.(13) and (C4), we obtain that the optimum coherent spin squeezing is given by Eq.(46).

Appendix D: Determination of the time t^* when the optimization direction of the Fisher information changes in the absence of noise

If the number N of atoms is even, the direction of optimization $\vec{n}_F^{(0)}$ of the Fisher information in a noiseless Bose Josephson junction is along x-axis at the time $t_2 = T/4$ of formation of the superposition of the two phase states $|\theta = \pi/2, \phi = 0\rangle$ and $|\theta = \pi/2, \phi = \pi\rangle$. These phase states are indeed diametrically opposite on the equator of Bloch sphere along this axis. Since $\vec{n}_F^{(0)}(\tau) = \vec{n}_+^{(0)}(\tau)$ is in the (yOz)-plane at times $\tau = 2\pi t/T \ll 1$ (see Sec.VA), the optimizing direction thus changes abruptly from the (yOz)-plane to the x-axis at some time $\tau^* \in]0, \pi/2[$ satisfying

$$\gamma_x^{(0)}(\tau^*) = \gamma_+^{(0)}(\tau^*). \qquad (D1)$$

In this appendix we determine τ^* explicitly in the limit of large total atom number N, supposed to be even. We may infer from the previous discussion that τ^* is neither close to 0 nor close to $\pi/2$. Consequently, we look for a solution of the implicit equation (D1) in the interval $\tau \in [N^{-\alpha}, \pi/2 - N^{-\alpha}]$, α being a positive exponent strictly smaller than $1/2$. Introducing the variables $u \equiv \cos(\tau) \in [0, \cos(N^{-\alpha})]$ and $v \equiv \cos(2\tau) \in [-\cos(2N^{-\alpha}), \cos(2N^{-\alpha})]$, we obtain with the help of Eqs.(43) and (44)

$$\frac{4(\gamma_+^{(0)}(\tau) - \gamma_x^{(0)}(\tau))}{N} = -(N-1)v^{N-2} + Nu^{2N-2} \qquad (D2)$$
$$+2(N-1)u^{2N-4}(1-u^2) + O(Nu^{4N-8}) + O(Nv^{2N-4}).$$

Setting $\gamma_+^{(0)}(\tau) = \gamma_x^{(0)}(\tau)$ gives the equation

$$\left(2-\frac{1}{u^2}\right)^{N-2} = 2 - u^2\frac{N-2}{N-1} + O(e^{-N^{1-2\alpha}}). \qquad (D3)$$

For large N, the right-hand side of Eq.(D3) is strictly larger than one and is of the order of unity. Hence the solution must satisfy $|2 - u^{-2}| > 1$ and $2 - u^{-2} \simeq \pm 1$. We may exclude the positive sign as the values $u = \pm 1$ correspond to $\tau \simeq 0$ or $\tau = \pi$ outside the studied time interval. The relevant solution u of Eq.(D3) is thus close to $1/\sqrt{3}$ and smaller than this number. Let us note that for odd N's, such a solution does not exist; indeed, in this case Eq.(D1) has no solution (see Sec.VA). Let us set $u = 1/(\sqrt{3}(1+\delta))$. Then from Eq.(D3) we obtain

$$e^{(N-2)\ln(1+6\delta+O(\delta^2))} = \frac{5}{3} + O(\delta) + O\left(\frac{1}{N}\right) \qquad (D4)$$

from which we find

$$\delta = \frac{1}{6N}\ln\left(\frac{5}{3}\right)\left(1+O\left(\frac{1}{N}\right)\right) \qquad (D5)$$

In terms of the dimensionless time τ^* we get

$$\tau^* = \arccos\left(\frac{1}{\sqrt{3}}\right) + \frac{\ln(5/3)}{6\sqrt{2}N} + O\left(\frac{1}{N^2}\right). \qquad (D6)$$

Appendix E: Analytical results for the spin-squeezing parameter and the quantum Fisher information in the large-N limit

Short time regime. At times shorter than the time of formation of the first macroscopic superpositions, ie $0 \leq t \ll t_{fs}$ (or $\tau \ll 1/\sqrt{N}$), one has $\gamma_+^{(0)}(t) > \gamma_x^{(0)}(t)$. A short-time expansion in Eq.(44) followed by the large N limit yields [46]

$$F_Q^{(0)}(\tau) = 4\gamma_+^{(0)}(\tau) \simeq N\left[1+\left(\frac{N^2\tau^2}{2}+N\tau\sqrt{1+\frac{N^2\tau^2}{4}}\right)\right]. \qquad (E1)$$

In this time regime, the visibility (41) is almost equal to one. In order to compare F_Q with $F_\xi = N/\xi^2$, we determine the ratio

$$\frac{F_Q^{(0)}(\tau)}{F_\xi^{(0)}(\tau)} \simeq \frac{N+1}{2} - \frac{N-1}{2}\cos^{N-2}(2\tau)$$
$$-(N-1)^2\cos^{2N-4}(\tau)\sin^2(\tau) \qquad (E2)$$

by employing Eq.(46) and identifying the product $\gamma_+^{(0)}(\tau)\gamma_-^{(0)}(\tau)$ with the determinant of the 2×2 submatrix $\gamma^{(0)'}(t)$ in Eq.(42). At short times $\tau \ll N^{-2/3}$, which a posteriori turns out to be the time of optimal squeezing, the RHS of Eq.(E2) can be approximated by one, yielding

$$F_\xi^{(0)}(\tau) \equiv \frac{N}{\xi^{(0)}(\tau)^2} \simeq F_Q^{(0)}(\tau) \qquad (E3)$$

as discussed in the main text. At later times $\tau \lesssim N^{-2/3}$ the right-hand side of Eq.(E2) can be approximated by $1 + N^4\tau^6/6$. We obtain [46]

$$\xi^{(0)}(\tau)^2 \simeq \frac{N(1 + N^4\tau^6/6)}{F_Q^{(0)}(\tau)} , \qquad (E4)$$

where $F_Q^{(0)}(\tau)$ is given by Eq.(E1) up to a relative correction $O(N^{-1/3})$. The squeezing parameter (E4) reaches a minimum $(\xi_{\min}^{(0)})^2 \simeq (3/N)^{2/3}/2$ at the time $\tau_{\min}^{(0)} = 3^{1/6}N^{-2/3}$ in the limit $N \gg 1$, as assumed above (see also Ref. [8] where a different definition of ξ is used, which however almost coincides with ours at times $t \ll t_{sf}$ because $\nu^{(0)}(t) \simeq 1$). The value of the Fisher information at $\tau = \tau_{\min}^{(0)}$ is $F_Q(\tau_{\min}^{(0)}) \simeq 3^{1/3}N^{5/3}$. The direction of optimization of F_Q is in the (yOz)-plane and is given by the eigenvector $n_+^{(0)}(\tau)$ orthogonal to $n_-^{(0)}(\tau)$, that is, $\phi_F^{(0)}(\tau) = 0$ and $\theta_F^{(0)}(\tau) = \theta_\xi^{(0)}(\tau) + \pi/2$. One finds by using the first equality in (48) that $\tan\theta_\xi^{(0)}(\tau) \simeq (N\tau/2 + \sqrt{1 + N^2\tau^2/4})^{-1}$. The angle $\theta_\xi^{(0)}$ starts from $\pi/4$ at $\tau = 0$ and quickly decreases to the value 0, to which it is almost equal at times $\tau \gg N^{-1}$. At such times ξ and F_Q are optimal along $\vec{e}_z$ and $\vec{e}_y$, respectively (see Eq.(47)). These results are summarized in Table II.

Intermediate times. In the time regime $\delta t \leq t \leq T/4 - \delta t$ with $\delta t \gg t_{fs}$, the covariance matrix (42) takes the simple following form in the limit $N \gg 1$

$$\gamma^{(0)}(\tau) \simeq \begin{pmatrix} \frac{1}{8}N(N+1) & 0 & 0 \\ 0 & \frac{1}{8}N(N+1) & 0 \\ 0 & 0 & \frac{1}{4}N \end{pmatrix} . \qquad (E5)$$

Hence the Fisher information has a plateau at the value

$$F_Q^{(0)}(\tau) = \frac{N(N+1)}{2} \qquad (E6)$$

whereas the squeezing parameter

$$F_\xi^{(0)}(\tau) \simeq N\nu^{(0)2}(\tau) \qquad (E7)$$

decreases with time as $\nu^{(0)}(t)$ decreases (second panel of Fig.4). We have shown in Appendix C that if N is even, the optimizing direction $\vec{n}_F^{(0)}(\tau)$ of the Fisher information changes as τ increases from the (yOz)-plane to the x-axis at the time $\tau^* \simeq \arccos(1/\sqrt{3})$ defined by $\gamma_x^{(0)}(\tau^*) = \gamma_+^{(0)}(\tau^*)$. Note, however, that any direction in the (xOy)-plane gives a Fisher information almost equal to the optimized value $N(N+1)/2$, as mentioned above and as it is clear from the structure of the matrix (E5). For an odd number of atoms N, the optimal direction $\vec{n}_F^{(0)}(\tau)$ remains in the (yOz)-plane all the way up to $\tau = \pi/2$ (i.e., $\gamma_x^{(0)}(\tau) < \gamma_+^{(0)}(\tau)$ for any $\tau \in [0, \pi/2]$). More precisely, it is almost along the y-axis (which is the symmetry axis of the superposition (19) formed at $t = t_2$) at times $N^{-1} \ll \tau \leq \pi/2$.

Times t close to $t_2 = T/4$. At times t such that $|t_2 - t| \ll T$, the Fisher information is given by

$$F_Q^{(0)}(\tau) \simeq \frac{N}{2}\left(N + 1 + (N-1)e^{-2N(\pi/2 - \tau)^2}\right) . \qquad (E8)$$

It increases monotonously from the plateau value (E6) at times $t \simeq T/4 - t_{sf}$ to the value N^2 at the time $t = t_2$ of formation of the two-component macroscopic superposition, which has the highest Fisher information $F_Q = N^2$ allowed by the Heisenberg bound. The optimal direction of F_Q is along the x-axis if N is even and the y-axis if N is odd, and that of ξ is along the z-axis in both cases.

Results in the presence of noise. The formula generalizing Eq.(E4) for small nonzero noise intensities $a(\tau) \lesssim N^{-1}$ reads

$$\xi^2(\tau) \simeq \frac{1 + N^4\tau^6/6 + N(\delta\lambda/\chi)^2\tau^2 + O(N^{-1/3})}{1 + \left(\frac{N^2\tau^2}{2} + N\tau\sqrt{1 + \frac{N^2\tau^2}{4}}\right)} , \qquad (E9)$$

where we assumed $\tau \lesssim N^{-2/3}$ and $\delta\lambda/\chi \lesssim N^{1/6}$. The minimum value of $\xi(\tau)^2$ is given by Eq.(55) of the main text. The angle θ_ξ which identifies the optimal squeezing direction satisfies $\tan(\theta_\xi) = e^{-a^2(t)/2}\tan(\theta_\xi^{(0)})$.

[1] C. Chin *et al*, Rev. Mod. Phys. **82**, 1225 (2010)
[2] J. Fortágh and C. Zimmermann, Rev. Mod. Phys. **79**, 235 (2007).
[3] I. Lesanovsky and W. Von Klitzing, Phys. Rev. Lett. **99**, 083001 (2007).
[4] J. Appel *et al*, Proc. Na. Ac. Sci. of United States of Am. **106**, 10960 (2009); W. Wasilewski *et al*, Phys. Rev. Lett. **104**, 133601 (2010).
[5] M.H. Schleier-Smith, I.D. Leroux, and V. Vuletic, Phys. Rev. Lett. **104**, 073604 (2010).
[6] C. Gross *et al*, Nature **464**, 1165 (2010).
[7] M.F. Riedel *et al*, Nature **464**, 1170 (2010).
[8] M. Kitagawa and M. Ueda, Phys. Rev. A **47**, 5138 (1993).
[9] A. Sorensen *et al*, Nature **409**, 63 (2001).
[10] D.J. Wineland *et al*, Phys. Rev. A **50**, 67 (1994).
[11] L. Pezzé and A. Smerzi, Phys. Rev. Lett. **102**, 100401 (2009).
[12] V. Giovannetti, S. Lloyd and L. Maccone, Phys. Rev. Lett. **96**, 010401 (2006).
[13] B. Yurke and D. Stoler, Phys. Rev. Lett. **57**, 13 (1986); D. Stoler, Phys. Rev. D **4**, 2309 (1971).

[14] G. Ferrini, A. Minguzzi and F.W.J. Hekking, Phys. Rev. A **78**, 023606 (2008).

[15] F. Piazza, L. Pezzé, A. Smerzi, Phys. Rev. A **78**, 051601 (2008).

[16] A. Sinatra and Y. Castin, Eur. Phys. J. D **4**, 247 (1998).

[17] J. Anglin, Phys. Rev. Lett. **79**, 6 (1997).

[18] D. Witthaut, F. Trimborn, and S. Wimberger, Phys. Rev. A **79**, 033621 (2009).

[19] Y. P Huang and M.G. Moore, Phys. Rev. A **73**, 023606 (2006).

[20] Y. Khodorkovsky, G. Kurizki, and A. Vardi, Phys. Rev. Lett. **100**, 220403 (2008).

[21] J. Esteve *et al*, Nature **455**, 1216 (2008).

[22] G. Ferrini *et al*, Phys. Rev. A **82**, 033621 (2010)

[23] S.L. Braunstein and C.M. Caves, Phys. Rev. Lett. **72**, 3439 (1994); V. Giovannetti, S. Lloyd, and L. Maccone, Phys. Rev. Lett. **96**, 010401 (2006)

[24] T.Kim *et al*, Phys. Rev. A **57**, 4004 (1998).

[25] B. Yurke, S.L. McCall, and J.R. Klauder, Phys. Rev. A **33**, 4033 (1986).

[26] W.M. Zhang, D.H. Feng and R. Gilmore, Rev. Mod. Phys. **62**, 867 (1990).

[27] A. Uhlmann, Rep. Math. Phys. **9**, 273 (1976)

[28] S.L. Braunstein, C.M. Caves and G.J. Milburn, Ann. Phys. **247**, 135 (1996).

[29] P. Hyllus, O. Güne, and A. Smerzi, Phys. Rev. A **82**, 012337 (2010).

[30] V. Giovannetti, S. Lloyd and L. Maccone, arXiv:1102.2318 (2011).

[31] G.J. Milburn *et al*, Phys. Rev. A **55**, 4318 (1997).

[32] D.S. Hall *et al*, Phys. Rev. Lett. **81**, 1539 (1998).

[33] J. Grond *et al*, arXiv:1010.3273 (2010).

[34] I. Tikhonenkov, M.G. Moore and A. Vardi, Phys. Rev. A **82**, 043624 (2010).

[35] C. Gross, Ph.D. thesis, Heidelberg (2010).

[36] L. Viola and S. Lloyd, Phys. Rev. A **58**, 2733 (1998).

[37] We focus on the effect of phase noise on the preparation of the useful input state. For studies of the effect of noise during the rotations or the measurements, see references [38] and [30].

[38] U. Dorner, arXiv:1102.1361 (2011).

[39] D. Giulini *et al*, *Decoherence and the appearance of a Classical World in Quantum Theory* (Springer, 1996).

[40] M. Orszag, *Quantum Optics*, 2nd ed. (Springer, 2008)

[41] G. Ferrini, A. Minguzzi, and F.W.J. Hekking, Phys. Rev. A **80**, 043628 (2009).

[42] F.T. Arecchi, E. Courtens, R. Gilmore, and H. Thomas, Phys. Rev. A **6**, 2211 (1972)

[43] A.R.U. Devi, X. Wang and B.C. Sanders, Quant. Inf. Proc. **2**, 207 (2003).

[44] We cannot exclude here that slightly different values of β would appear for larger N's.

[45] For the chosen interval of noise strengths, the analysis of the scaling $F_Q = cN^\beta$ is meaningful as the multiplying constant c, which also depends on the noise, is large enough to ensure that $F_Q(t_{\max}) \gg N$, as shown in the first panel in Fig.8.

[46] We use $1 - \cos^{N-2}(2\tau) \simeq 2N\tau^2 - 2N^2\tau^4 + 4N^3\tau^6/3$ and $(N-1)\cos^{2N-4}(\tau)\sin^2(\tau) \simeq N\tau^2 - N^2\tau^4 + N^3\tau^6/2$.

[47] $a_{\mathrm{echo}}^2(t)$ is positive since $h''(0) < 0$. This follows from the fact that the correlation function h is of positive type and hence has a positive Fourier transform.